The Effects of Varying Winter Surface Heat Loss on the Labrador Sea Water and Its Export

MSc Thesis for the Hydraulic Engineering Department

F.M.B. Kollaard

2022

TU Delft

The effects of varying winter surface heat loss on the Labrador Sea Water and its export

by

Freek Kollaard

In partial fulfilment of the requirements for the degree of

Master of Science
in Hydraulic Engineering

at the Delft University of Technology,
to be defended publicly on Monday July 4, 2022 at 15:00 UTC+1.

Thesis committee:

Prof. dr. Caroline Katsman,	TU Delft, Chair
Prof. dr. Julie Pietrzak,	TU Delft
Dr. Stephan de Roode,	TU Delft

Student number: 4369572
Department of Hydraulic Engineering
Faculty of Civil Engineering and Geosciences
Delft University of Technology

TU Delft

Abstract

As the environment is changing temperatures are changing, becoming more extreme. This is expected to affect the oceans and its transport, specifically the Atlantic Meridional Overturning Circulation (AMOC). The Labrador Sea is a part of the AMOC, where overturning in depth and density space occurs, due to deep convection. Deep convection is the process of seawater losing its heat to the atmosphere, due to atmospheric cooling during the winter. This causes the seawater to become colder and denser, and it therefore sinks towards the bottom of the basin. Deep convection is previously studied extensively as it is a unique and important process of the global ocean circulation system. The key process that causes the AMOC water to overturn, is due to buoyant eddies shedding from the boundary current into the interior. The buoyant eddies exchange their buoyant boundary current water with the dense interior water, causing the boundary current (and in extension the AMOC water) to cool down.

Previous studies have shown that the properties of the boundary current water are strongly dependent on the eddy exchange, and therefore on the surface heat loss. However, it is not known how consecutive strong winters impact the dynamics of the Labrador Sea on various timescales, which will therefore be the focus of this thesis. Data for this research will be obtained by using an idealised model configuration of the Labrador Sea, where the hydrostatic primitive equations of motion are solved by the MIT general circulation model (MITgcm). Different types of scenarios are defined to analyse different effects on the dynamics. These scenarios are analysed by looking into how the mean basin temperature changes, how the eddy kinetic energy (EKE) and mixed layer depth (MLD) develop, and how the properties through a transect of the basin change. The effects of these interactions are then studied by looking at how the transport of water throughout the boundary current, per density class and per vertical layer change.

The thesis mainly shows that the mixed layer depth in the interior increases during a strong winter. As a result, the eddy kinetic energy increases significantly in the boundary current, as the horizontal density gradient increases, thus causing an increase in boundary current velocity in the downstream direction. Additionally, more and denser interior water accumulates, depending on how many consecutive strong winters occur. This deep convected water in the interior partly remains near the bottom of the basin. In the next winter, it is mixed again due to deep convection, consequently a positive feedback loop occurs. Meaning, that the number of consecutive winters positively impacts the interactions in the basin, as the horizontal density gradient increases, and thus the velocity and eddy kinetic energy increase as well, in respect to the previous winter. The effect of the strong winters persists in the years afterwards, as the interior remains relatively cold. Additionally, a part of the accumulated convected interior water resides too deep in the basin to be exchanged by the eddy exchange and therefore flows near the bottom out of the basin, due to a pressure difference. The flow near the bottom is a negative feedback loop, as the volume of dense convected water decreases and can therefore not be further cooled during consecutive strong winters. Finally, the properties and the transport of the boundary current water are directly related to the interior water and eddy exchange. As the MLD in the interior and eddies in the BC are still relatively large in the years after the additional surface heat loss, the export of boundary current water therefore also remains affected. In conclusion, the effect of wintertime surface heat loss on the Labrador Sea Water in the short term has the most influence on the MLD and EKE, however the influence of the MLD and EKE remains and therefore in the long term affects the export through the BC. These conclusions can help to better interpret the limited available measurements of the Labrador Sea Water.

Table of Contents

1 | Introduction

This chapter introduces the problem that is studied in this thesis. It starts with general background information about the Labrador Sea and why it is an area of interest (Section 1.1). Next, the important physical processes in the Labrador Sea are discussed (Section 1.2). Then, previous research is discussed to determine if there are gaps in current knowledge and what could be added to resolve this (Section 1.3). Next, the focus of this thesis is discussed and a research question and a series of sub-questions are formulated (Section 1.4). Finally, the structure of the thesis is discussed (Section 1.5).

1.1 Understanding the AMOC and its relevance

As the environment is changing temperatures are changing, becoming more extreme; this also affects the ocean and therefore its transport. One of the most important heat transport systems on earth is the Atlantic Meridional Overturning Circulation (AMOC). The AMOC transport is both wind-driven and thermohaline-driven. Water is heated at the equator causing the water to become saltier due to evaporation. This water, schematised as the red arrow in Figure 1.1a, flows northwards through the Atlantic Ocean, gradually releasing heat to the atmosphere, causing a relatively warm climate in the Northern Hemisphere. Due to the gradual release of heat to the atmosphere, this water cools as it travels toward the polar regions. In the subpolar and polar regions, the water becomes even denser due to strong surface heat loss and mixes vertically with deep water layers (Marshall & Schott, 1999). This transformation of water density is called deep convection, and there are only a few regions in the ocean where this occurs, including the Labrador Sea (Figure 1.1a encircled in red). The resulting dense water travels through deep regions southwards, schematised as a blue arrow in Figure 1.1a.

Currently, the strength of the AMOC is in the weakest state since recent decades (Caesar et al., 2021). As the strength of the AMOC decreases the redistribution of heat over the world changes. This could for instance cause a general cooling of the Northern Hemisphere, an increase in the number of North Atlantic storms, or large changes in precipitation in the tropics (Jackson et al., 2015). Thus having large implications for the climate over the whole world and should therefore be researched extensively. Unfortunately, the AMOC is difficult to measure, as the water velocity is very low (in the order of mm/s) and the areas through which the AMOC flows are very large. Nonetheless, measuring stations are situated at the inflow and outflow of the Labrador Sea (Holliday et al., 2018), but these provide limited insight into what happens inside the Labrador Sea. Without a detailed understanding of the processes governing the Labrador Sea Water (LSW), it is therefore difficult to make future predictions about how the AMOC might change. Thus, it is in our interest to study the deep convection regions of the Labrador Sea and how they react to (large) temperature fluctuations. In this thesis, the focus is therefore on applying a numerical model to simulate the Labrador Sea and interpret how the dynamics inside the Labrador Sea are affected, and therefore affect the AMOC.

1.2 Driving forces of the formation and export of Labrador Sea Water

To fully understand the driving forces of the Labrador Sea, each process is explained in this section in detail. Generally, the Labrador Sea can be described by a strong cyclonic boundary current (BC), and a quiescent interior (Lavender et al., 2000). Where the BC is characterised as a warm buoyant inflow and denser deeper outflow, with a dense interior. The Labrador Sea BC is driven by a subpolar wind-driven gyre and by the geostrophic and hydrostatic thermal wind balance, as seen in Equation 1.1,

$$f\frac{\partial \overrightarrow{u}}{\partial z} = \frac{g}{\rho_0}\nabla_h \rho \tag{1.1}$$

where f is the Coriolis parameter, $\overrightarrow{u}$ is the horizontal flow component, g is the gravitational acceleration, ∇_h is the horizontal gradient operator and ρ is the density. This balance indicates that an increase in lateral density gradient causes an increase in the velocity of the BC in the downstream direction. As the interior is denser than the BC, it therefore has a large lateral density gradient, thus enhancing the BC velocity.

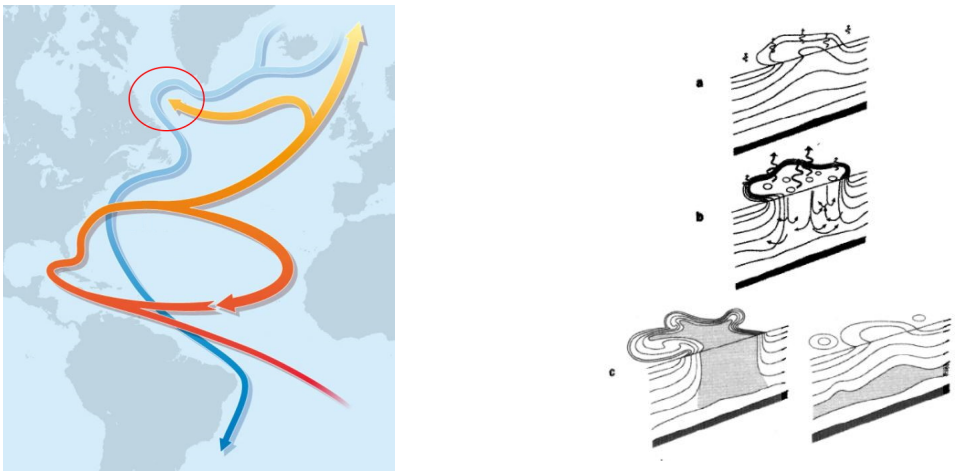

(a) (b)

Figure 1.1: a) Schematic of the Atlantic Meridional Overturning Circulation. The red encircled area is the Labrador Sea. Relatively warm water (red arrow) flows northwards through the upper layers of the Atlantic Ocean. Relatively cold water (blue arrow) flows southwards through deeper layers (Marotzke, 2012). b) Schematic diagram of the three phases of open- ocean deep convection: (a) preconditioning, (b) deep convection, and (c) lateral exchange and spreading. (Marshall & Schott, 1999)

The dynamics of the Labrador Sea are schematised in Figure 1.2a. Johnson et al. (2019) schematises the incoming buoyant water of the AMOC into the Labrador Sea as a. The process of deep convection takes place in the middle of the Labrador Sea (schematised as c) and is a result of atmospheric cooling during the winter (schematised as b). Therefore the interior water is relatively dense. The process of deep convection is best described in three phases and is illustrated in Figure 1.1b. The first phase consists of a negative surface heat flux applied to a body of water during winter. In the second phase, the water body loses heat to the atmosphere and the previously stratified structure is dissolved into multiple convective plumes. Which causes the properties of the water to mix, forming a large mixed volume of water. In the third phase, the volume of the mixed water is dispersed due to gravity and rotation outwards along the isopycnal (Marshall & Schott, 1999). This water will no longer be in contact with the atmosphere and therefore it is difficult to add or extract buoyancy. Thus without an external energy source, this water will not be able to increase or decrease in density and therefore will not be able to cross isopycnals.

The transformation of incoming buoyant BC water into dense outflowing water (schematised as e), is attributed to two processes. The atmospheric cooling in the winter does not only affect the interior, but the BC is also affected, and it therefore loses buoyancy. The second feature is due to an eddy exchange, in the eastern side of the Labrador sea near the Greenland coast, between the BC and the interior (schematised as d). The eddies are formed along the edge of Greenland, due to a narrowing of the topography, causing the BC to become unstable and large (Lilly et al., 2003; Katsman et al., 2004). These eddies shed buoyant water from the BC into the interior and due to mass conservation, an equal amount of dense interior water is transported along the isopycnals back into the BC. This eddy exchange is highlighted in Figure 1.2b. Brüggemann & Katsman (2019) highlights that the BC surface water is able to transform into denser water due to atmospheric cooling. Additionally, it shows that the water from the eddies shedding from the top layers of the BC into the interior is vertically mixed due to deep convection in the interior. Which causes this water to transform into deeper denser layers, and flow back into the BC along the isopycnals the BC, due to mass conservation. In summary, the combination of surface heat loss over the entire basin, deep convection in the interior, and the eddy exchange between BC and interior results in the densification of the BC while flowing through the Labrador Sea.

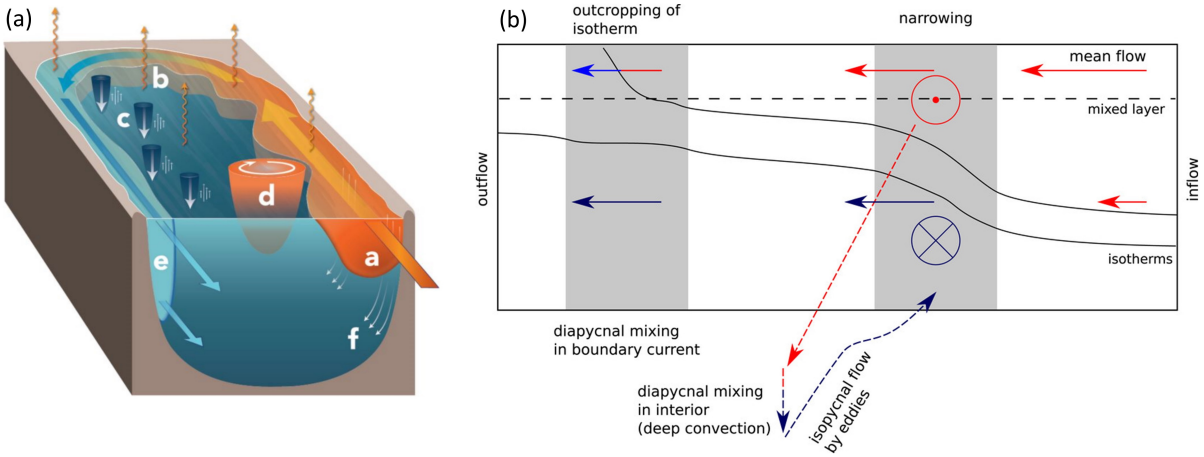

Figure 1.2: a) Schematic illustrating the key circulation features operating in North Atlantic marginal seas, like the Labrador Sea, where dense water formation occurs: (a) warm inflowing BC, (b) buoyancy loss to the atmosphere, (c) convective plumes, (d) buoyant eddies shed from the BC, (e) cooler outflowing BC, and (f) downwelling along the topography, from (Johnson et al., 2019)
b) Schematic of how strong eddy activity affects the Labrador Sea. It reflects 1) Water mass transformation in the upper part of the boundary current where the warmer layers outcrop to the surface. 2) Water mass transformation in the interior by deep convection, where a lateral connection between the convection sites and the boundary current by an isopycnal eddy flow along tilted isopycnals is essential to close the overturning loop, from (Brüggemann & Katsman, 2019)

1.3 Previous studies about processes governing the Labrador Sea Water

The AMOC is difficult to measure, as it has a large year-to-year variability and flows on large time and spatial scales. Furthermore, the Labrador Sea dynamics are equally difficult to measure, as the eddies shedding from the BC are highly variable and also are shed out of the BC over a large area. However, Holliday et al. (2018) present Eulerian measurements of the transport and density structure at the inflow and outflow of the Labrador Sea. These measuring stations are located at the West Greenland Current (WGC) and at the outflow at the Labrador Current (LC) (Figure 1.3). The Eulerian measurements monitor the net effect of the processes inside the Labrador Sea. Thus, it gives insight into how the AMOC changes in depth and density space, but it does not give insight into how the Labrador Sea dynamics are affected. These measurements are useful to gain more insight into how the system behaves on the mesoscale, without specifically measuring all interactions. Idealised numerical models are therefore used to gain insight into how the dynamics inside the Labrador Sea are affected. Thus, by comparing numerical model results of the dynamics inside the Labrador Sea, with the measurements of OSNAP at the inflow and outflow, the formation of LSW can be better understood.

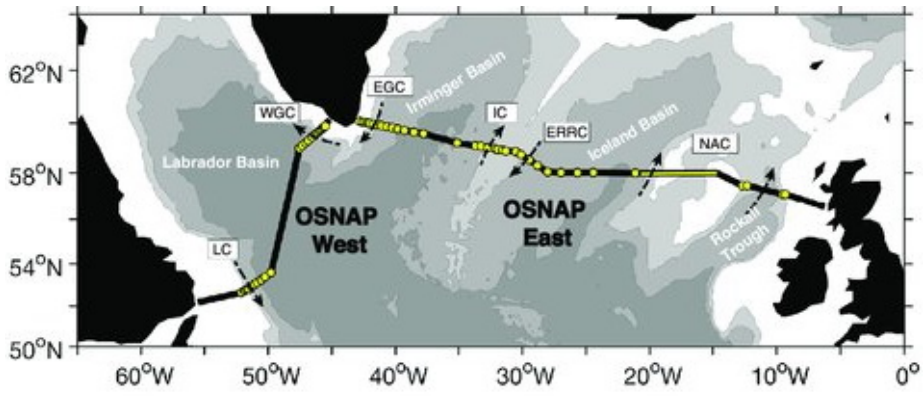

Figure 1.3: The locations of the OSNAP measurements stations for the Labrador Sea. The inflowing BC is located at the West Greenland Current (WGC) and the outflow is at Labrador Current (LC). (Li et al., 2021)

The densification of the BC is mainly attributed to the combination of deep convection in the interior and the eddy exchange between the BC and interior (Figure 1.2a). Deep convection is an important process in the formation of LSW and is therefore researched extensively. A relatively new study that tries to better understand the dynamics of the Labrador Sea is done by Georgiou et al. (2020). One of their main objectives is to provide a better understanding of the important interactions in the Labrador Sea. Specifically how changes in the surface heat flux, influences the convection, eddy activity and the magnitude of downwelling. In conclusion, it emphasizes the importance of the interaction between the BC and the interior through eddy activity. It shows that the response of the Labrador Sea dynamics to changes in atmospheric forcing is indirect mainly due to the eddy activity. One of the topics that led to this conclusion was a series of numerical simulations, where the atmospheric cooling in the wintertime is changed by 50% with respect to a reference run, which is defined as an average winter. (From this point on, this average reference run is dubbed as REFG.) This change in wintertime cooling is a continuous forcing over the entire simulation period and is therefore focused on the long-term response of the Labrador Sea dynamics. However, climate change does not only cause a constant change in mean wintertime atmospheric cooling, but it also causes more extremities in both summers and winters. Therefore the main goal of this study is to gain more insight into how the processes inside the Labrador Sea are affected by a varying increase in atmospheric cooling during the winter, instead of a continuous increase in atmospheric cooling (Georgiou et al., 2020). By comparing these results to the measurements of OSNAP (Holliday et al., 2018), the timing and location of these measurements could be improved, however it is not the goal to model it one to one with reality.

1.4 Research question

The goal of this study is to further investigate how the processes governing the Labrador Sea are affected by wintertime heat loss. This is done by using an idealized numerical model and periodically increasing the atmospheric cooling over the Labrador Sea (which is further explained in the Chapter 2) and investigating governing processes of the LSW are affected. Therefore the following research question is formulated:

How do consecutive severe winters influence the composition and export of Labrador Sea Water?

To be able to answer the main research question, it is subdivided into the following sub-questions:

1. How do the processes governing the Labrador Sea Water (boundary current- convection- and eddy field), adjust to the wintertime heat loss?

2. Considering the adjustment times of the dynamics, do the changes in dynamics scale with the duration and intensity of extreme wintertime heat loss?

3. Can the results of the idealised model help to interpret variability in Labrador Sea Water export, as seen in observations?

1.5 Thesis outline

In this thesis, the Method is formulated in Chapter 2, where the numerical model is described and how it is set-up in Section 2.1. Then is explained what type of runs are made to address the research question (Section 2.2), and how these runs are studied to address the research question (Section 2.3). The runs are categorised based on the research goals, namely: 'consecutive strong winter runs', 'varying HL intensity runs' and 'combination runs'. The results of the first two scenarios are presented one at a time, starting with the varying time series runs in Chapter 3. Then the results of the intensity based runs are given in Chapter 4. In Chapter 5 the influence of surface heat loss on the seasonality is studied. The thesis is concluded by the Discussion and Conclusion in Chapter 6.

2 | Method

In this chapter, the approach of the research is explained. First, the applied numerical model for this research is introduced (Section 2.1). Additionally, an explanation follows on how it is set-up and what the properties are of the idealised configuration. In Section 2.2 is explained what types of scenarios are modelled and how much atmospheric cooling is applied. Next is explained how the results of these simulated scenarios are studied (Section 2.3).

2.1 The MIT general circulation model

In this section, the idealized model configuration for the Labrador Sea is introduced. The MIT general circulation model (MITgcm) is used in oceanic research, by numerically solving the incompressible Navier-Stokes equations. An idealized configuration of the Labrador Sea is simulated on the MITgcm, which is built on earlier work of Katsman et al. (2004), Gelderloos et al. (2011) and Georgiou et al. (2020). The emphasis is on the most important physical properties incorporated in the model and what variables are different in relation to the set-up of Georgiou et al. (2020). The configuration of the current model setup used in this study captures the physical processes that are essential to the cycle of convection and restratification in the Labrador Sea and hence is suited for this type of process study. The model domain covers the Labrador Sea only (Figure 2.1b). These are 1575 km in the meridional direction, 1215 km in the zonal direction and has a maximum depth of 3000 m. The model has a grid resolution of 3.75 km in the x and y-direction. In the z-direction there are 40 layers, which vary from 20 m at the top layer to 200 m at the bottom layer.

There are two open boundaries at the east and south boundary, through which the BC is forced, the other boundaries are closed. This is seen in Figure 2.1b, the open boundaries (approximately 100 km wide) are located in the east and in the southwest (locations indicated by arrows). All other boundaries are closed. The BC that flows through the two open boundaries is set equal to each other. This implies that there is conservation of mass in the system. It should be noted that this does not imply that there is also conservation of energy in the domain, as the temperatures of the outflowing water is not prescribed. In reality, the incoming (eastern) BC in the upper layers has cold fresh water and in the bottom layers warm salty water. However, the salinity is neglected in this study as observations show that the eddy structure is dominated by temperature effects (Lilly & Rhines (2002), Pickart et al. (2002)). Additionally, the main objective of this study is on understanding the dynamics in the Labrador Sea, not on detailed quantification. Thus, the stratification of the BC at the inflow is derived from a measured density structure and is converted to a temperature structure with a linear equation of state. This means that cold water is situated at the bottom and warm water at the top of the BC. Seasonal variations of the BC are included. Furthermore, this configuration includes the topographic narrowing near Greenland, which results in the shedding of Irminger rings from the BC into the interior. The model also incorporates seasonal variations of both the surface forcing and the BC and enhanced vertical resolution (Georgiou et al., 2020).

Average winter months are defined in Georgiou et al. (2020) by a reference year and are based on observations ((Yu et al., 2008)). The pattern of the observed surface heat flux is applied to the area of the model in Figure 2.1b. The water in the western part of the basin has the lowest surface heat flux, as can be seen in Figure 2.1b in darkest blue. A mean negative surface heat flux indicates that the sea surface is cooling. The surface heat flux is time-dependent, during summer months a positive surface heat flux is observed. The summer heat flux in this study is uniform, while the winter heat flux is amplified during certain years. This is further explained in Section 2.2.

The simulations are performed using the hydrostatic version of MITgcm. The model solves the hydrostatic primitive equations (HPE) of motion, which are based on a number of assumptions. First, the water is assumed to be incompressible. The hydrostatic assumption is valid, as the x and y domain size are far greater than the depth of the basin. Next, the Boussinesq assumption is used as the differences in the Labrador Sea Water density in respect to the average density is small. Furthermore, a Cartesian grid is assumed, as the curvature of the earth is negligibly small over the simulated domain. The Coriolis force is parameterised by applying the β-plane approximation, which is appropriate for the domain size considered. When an instability in stratification occurs, a convective adjustment scheme is applied, and convection is parameterized with implicit vertical diffusion (Kv = $10m^2/s$, instead of 0). MITgcm applies

Large Eddy Simulation (LES) to resolve eddies that are larger than the grid size. Based on an extensive study on the eddies shedding from the BC in the Labrador Sea, Lilly et al. (2003) found that the eddies have a radius from 5-30 km and are therefore well above the grid resolution of 3.75 km, used in this study. Horizontal biharmonic eddy viscosity is applied to help resolve the subgrid-scale motions. In this study, a higher Laplacian viscosity (viscAh = 40 m^2/s, instead of 10 m^2/s) and Laplacian diffusivity (diffKhT = 20 m^2/s instead of 5 m^2/s) are applied, than is allowed for a grid resolution of 3.75 km. However, the model becomes numerically unstable when the lower viscosity and diffusivity is applied in combination with additional wintertime heat loss. Although this solution to resolve the numerical instability is not perfect, it does not affect the large-scale eddies significantly (Griffies & Hallberg, 2000). Furthermore, in Georgiou et al. (2020), the Laplacian viscosity and diffusivity are set to zero, which is also not the ideal solution, however this solution suits the goals of the type of study. This also applies for this study, as it is not the goal to model reality perfectly, but to qualitatively study how changes in wintertime heat loss affect the Labrador Sea Water. Values of all parameters used in 3yrDoubleHL can be found in Figure A.1.

Finally, the model exports four variables, the velocities in the x,y and z-direction, and the potential temperature. Every 2 days a snapshot of these variables is saved and a time average of every month is saved.

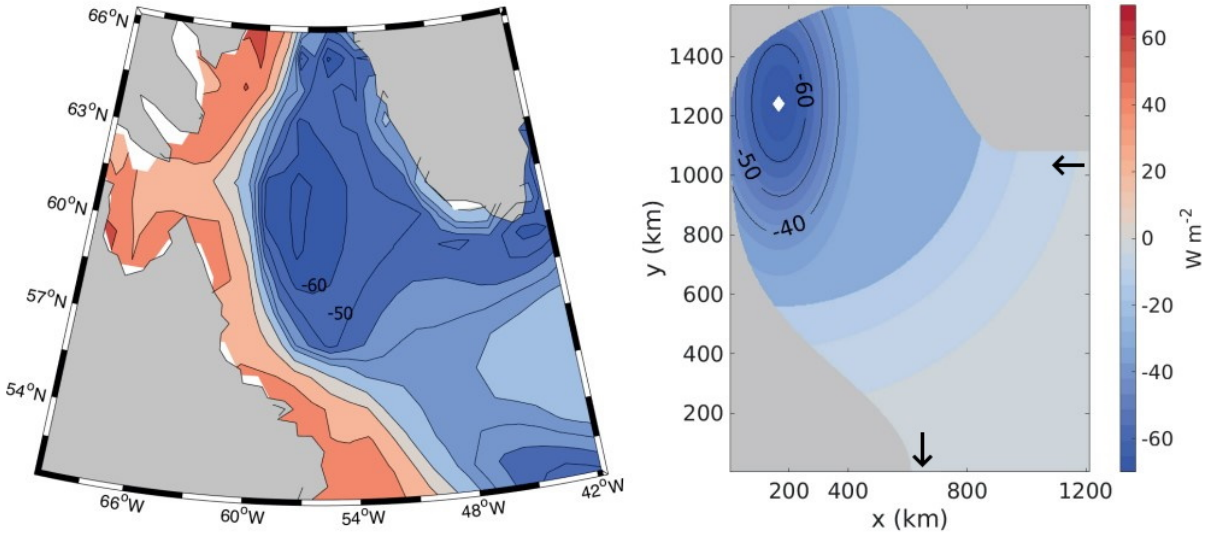

Figure 2.1: a) The mean surface heat flux (in W/m^2) from the years 1983 to 2009 (Yu et al., 2008). b) The idealized annual mean heat flux applied to the model, used as a reference year in this study. The white marker indicates the location where the maximum heat flux is applied. The arrows approximate the open boundaries, from (Georgiou et al., 2020)

2.2 Type of scenarios and forcing

In this section a number of runs are introduced and are categorised in scenarios, to help answer the research questions. The focus of this study is on how the processes inside the Labrador Sea are affected by a varying increase in atmospheric cooling during the winter, instead of a continuous increase in atmospheric cooling. Therefore the runs categorised in the first scenario focus on varying the amount of strong consecutive winters, with the aim to study how the consecutive strong winters change the dynamics of the Labrador Sea, in respect to the reference run. In these runs, the wintertime heat loss is doubled in respect to an average (reference) winter year. The annual forcing of the reference run is based on Figure 2.2 (and is also used in Georgiou et al. (2020)), which represents the averaged annual net surface heat flux over the Labrador sea, as a red line. The difference between an average winter and a strong winter is defined as a doubling of the average annual surface heat loss. The additional surface heat loss is only applied during the winter months, no changes in heat loss during the summer are made. This results in the runs 1yrDoubleHL (Figure 2.3a), 3yrDoubleHL (Figure 2.3b) and 5yrDoubleHL (Figure 2.3c) and are categorised as the 'consecutive strong winter runs'. Each run starts with 10 years of average heat loss to stabilise the system, based on the reference run of Georgiou et al. (2020), which has different viscosity and diffusivity values (as described in Section 2.1). Then in the first winter months (month 10 of year 11, to month 3 of year 12) the surface heat loss is doubled, compared to the average surface heat loss (for

1yrDoubleHL). In 3yrDoubleHL and 5yrDoubleHL the doubling of the average surface heat loss is done respectively for 3 and 5 consecutive winters. Each run ends with 5 years of average heat loss.

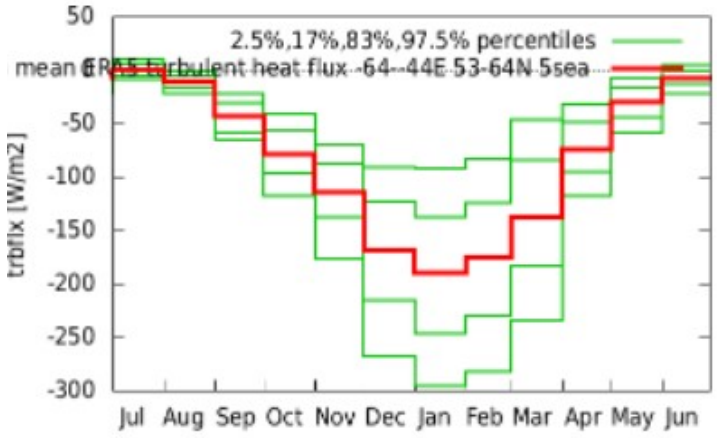

Figure 2.2: Averaged annual cycles of the net surface heat flux over the Labrador Sea (red line), defined as the area between 64W - 44W and 53-64N, computed with reanalysis data from 1950 to 2022. The green lines depict the percentiles of the average annual net surface heat flux, from (Hersbach et al., 2020).

The runs categorised by the second scenario focus on varying the intensity of a strong winter, with the aim to study how this variation in intensity changes the dynamics of the Labrador Sea, in respect to the reference run. The scenario is called the 'varying heat loss intensity runs' and consists of 1yrDoubleHL (Figure 2.3a) and 1yrTripleHL (Figure 2.3d). These runs are set-up similarly as the runs from the consecutive winter runs scenarios, but 1yrTripleHL has instead of a single year of doubling, a tripling of average surface heat loss during the first winter. Finally, a scenario that combines both of the aforementioned scenarios is called the 'combination runs', and contains two runs called AltDoubleHL and AltTripleHL. These two runs are similarly set-up as the previous runs, but instead have two strong winters with an average winter in between the strong winter years, and respectively have a doubling and tripling of average surface heat loss. The goal of this scenario is to give the basin time in between strong winters to recover from the additional surface heat loss. However, the results of AltDoubleHL and AltTripleHL are not further studied from this point onwards, as no differences are observed in these runs compared to the other scenarios. All the different runs are summarised in Table 2.1.

Table 2.1: An overview of the runs analysed in this study. Every run begins with 10 years of average heat loss to stabilise the system, based on the reference run from (Georgiou et al., 2020) (called REFG in this thesis). Different forcing times and intensities are applied, with each run ending with 5 years of average heat loss.

Name of run	Scenario	Type of forcing
REF	Reference	10 years REFG - 10 years average HL
1yrDoubleHL	Consecutive strong winters Varying HL intensity	10 years REFG – 1 year +100% heat loss – 5 years REF
3yrDoubleHL	Consecutive strong winters	10 years REFG – 3 years +100% heat loss – 5 years REF
5yrDoubleHL	Consecutive strong winters	10 years REFG – 5 years +100% heat loss – 5 years REF
1yrTripleHL	Varying HL intensity	10 years REFG – 1 year +200% heat loss – 5 years REF
AltDoubleHL	Combination	10 years REFG - 1 year +100% heat loss - 1 year - 1 year +100% heat loss - 5 years REF
AltTripleHL	Combination	10 years REFG - 1 year +200% heat loss - 1 year REF - 1 year +200% heat loss - 5 years REF

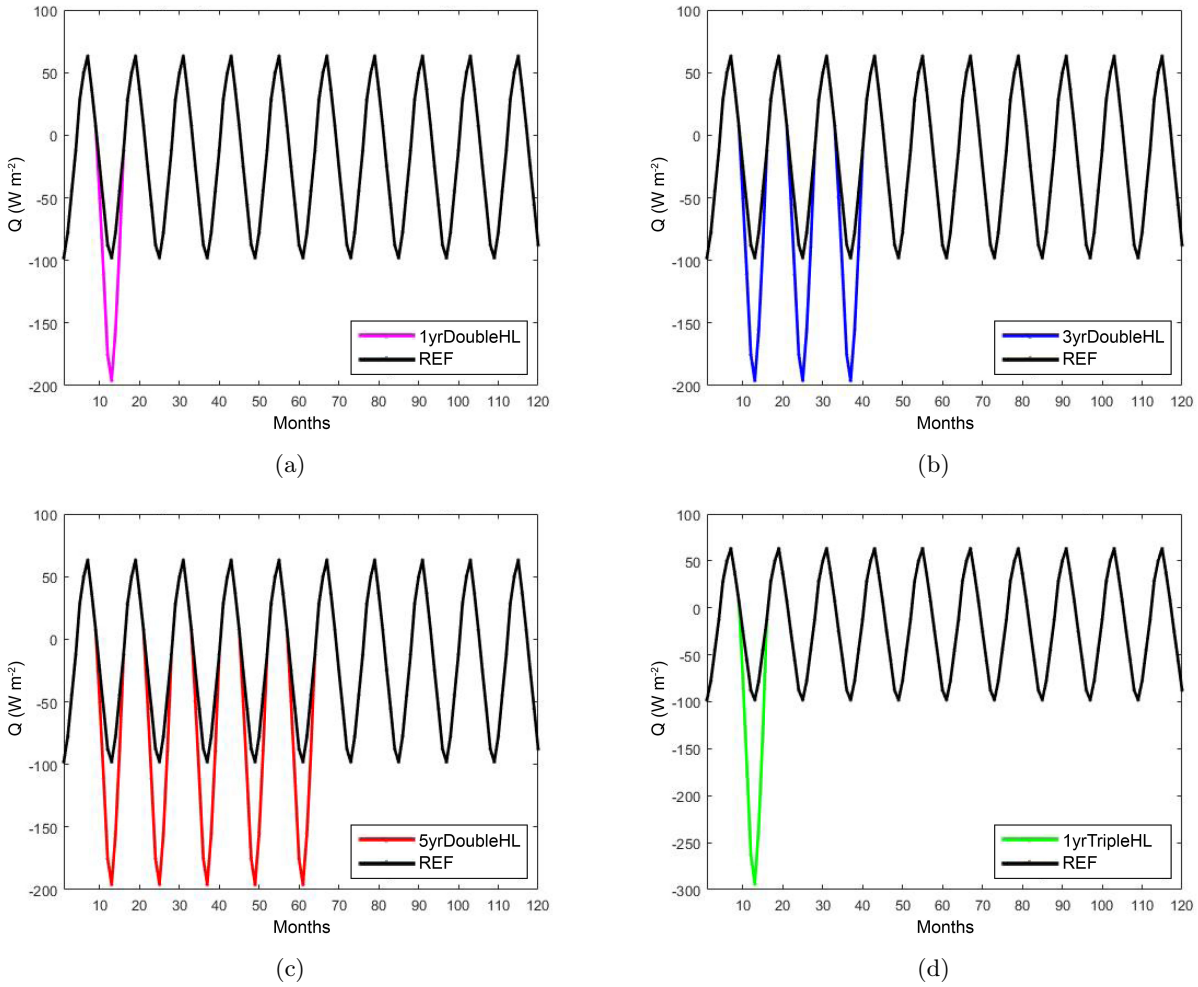

Figure 2.3: The seasonal cycles of the applied maximum surface heat flux (in W/m^2) over the simulation period, applied at the location as indicated by the white marker in Figure 2.1b, for a) 1yrDoubleHL, b) 3yrDoubleHL, c) 5yrDoubleHL and d) 1yrTripleHL.

2.3 Studying the results of the scenarios

In this section the type of scenarios are explained and how the results of the scenarios in Table 2.1 are studied. First, the mean basin temperature is discussed in Subsection 2.3.a. Then the EKE and MLD in Subsection 2.3.b, and properties through the basin in Subsection 2.3.c are discussed. Finally, the BC transport per vertical layer and per density class is discussed in Subsection 2.3.d. By studying these results it is expected to give more insight into how the dynamics of the Labrador Sea are affected by additional surface heat loss.

2.3.a Mean basin temperature

The first variable studied is the mean basin temperature. The runs from Table 2.1 are plotted as the mean temperature of the basin, that change over the simulation period. These runs are compared to the reference run, and REFG, to see how large the deviation is due to the additional wintertime forcing. This plot shows on the basin scale, how the system reacts to atmospheric cooling. The monthly time-averaged temperature from the model is used to calculate the mean basin temperature.

The goal of this plot is to get a first impression if the model reacts to the imposed seasonal variations. This includes looking into time dependencies, such as delays in the system, and investigating time-dependent trends due to the additional atmospheric cooling. The main process that influences the mean basin temperature is the surface heat loss during the winter months and the eddy exchange with the BC (Figure 1.2a. These are further discussed in Subsection 2.3.b.

2.3.b Eddy kinetic energy and mixed layer depth

As highlighted in Section 1.2 the eddy field near Greenland, has a large influence on the interaction between the BC and the interior, and is the key to exchanging BC water with deep convected water. This has been discussed in Chapter 1, which explains how the BC becomes colder due to the eddy exchange, forcing warm water from the BC into the interior, and cold water from the interior back into the BC. To study the eddy field, it is quantified as the surface eddy kinetic energy (EKE). The EKE (in cm^2/s^2) is described by the surface turbulent velocity components and is calculated by the following formula:

$$EKE = \frac{1}{2}\overline{(u')^2} + \overline{(v')^2} \tag{2.1}$$

Where u' and v' are the turbulent velocity components, derived from:

$$u' = u - \overline{u}, v' = v - \overline{v}, \tag{2.2}$$

which is the difference between the instantaneous velocity (u) and the average yearly velocity ($\overline{u}$). The velocities used to calculate the EKE are from the model and are based on the snapshot values that are saved every 2 days.

The mixed layer depth (MLD) is another metric to study the effects of oceanic heat loss. The MLD is the monthly averaged depth, where the density difference compared to the surface is $\rho = 0.005 kg/m^3$ (Courtois et al., 2017). Yashayaev & Loder (2017) has shown that during strong winters the MLD in the Labrador Sea can extend beyond depths of 2100 m. By studying how this variable changes, it can indicate where the convected water is and gives an indication of how much water is convected. Additionally, the MLD and EKE influence each other directly. An increased MLD in the eddy field could negatively influence the ability of eddies to penetrate into the interior, as they need additional energy to penetrate an area of higher density. Therefore looking into both EKE and MLD together, it can indicate if the interior water is able to exchange with the BC.

The EKE and MLD are analysed every year. The MLD values are based on the density difference compared to the surface water, therefore it uses the exported temperature values of the 2-day snapshots. The results from the months February and March are averaged to get the final MLD and EKE plot. This is because the meteorological winter months are in December, January and February, but the MLD has a lagged response. As is seen in Figure 1.1b in phase a) the water needs to cool for a period before it becomes dense enough to sink to greater depths. In the months February and March the surface of the interior has had sufficient time to cool, and is therefore chosen as the months to study the MLD.

From this point forward, when a reference is made to the winter months, it refers to the months February and March.

2.3.c Properties across the basin

To further study the dynamics of the Labrador Sea a transect is made through the middle (center blue line in Figure 2.4). The location of the transect is chosen through the area with large winter surface heat loss, as seen in Figure 2.1, to be able to study the deep convection. Additionally, the transect goes through the eddy field and can therefore give insight into how the eddies interact with the interior. And finally, the eastern and western BC are included, to be able to gain insight into the property differences on each side.

The goal of this plot is to study how the density structure develops in the winter months. This is done by plotting the isopycnals (in kg/m^3), in the winter months of every year. It further substantiates the results of the EKE and MLD, as it shows how the convected water is spread throughout the transect. Additionally, by plotting it for each year it can be seen how water with specific density classes are affected, and if the isopycnals are in contact with the BC. Furthermore, the velocity profile perpendicular to the transect is studied. The velocity profile is especially interesting in the eastern and western BC, as the velocity could give an indication of the export timescale of BC water. Furthermore, the velocity in the BC directly impacts the eddy formation, and therefore the amount of exchanged water.

All variables from the transect are based on the monthly average values of velocities and temperatures.

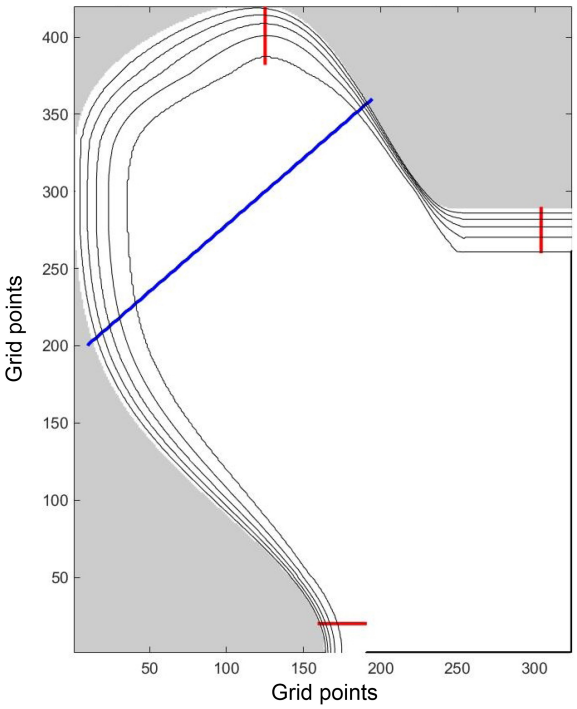

Figure 2.4: Model domain transect and sections used for BC analyses. The transect through the convection area is shown as a blue line. The red lines are the inflow, central and outflow transects. The depth is defined in black contour lines, defined at intervals of 500 m, down to 2500 m. The numerically closed boundaries of the basin are depicted by a thick black line in the southern and eastern side of the basin. The x and y-axis is defined as number of grids points, each grid box is 3.75km by 3.75 km.

2.3.d Boundary current transport per vertical layer and density class

After studying the MLD, EKE and properties of the Labrador Sea, the effect on the density structure of the BC is investigated. This is done by studying two segments of the BC, a segment between the inflow and central transect, and a segment between the central transect and outflow. These segments are defined by red lines in Figure 2.4. The in- and outflow segments are chosen 20 grid lengths away from the domain edges, to avoid interactions with the imposed boundary conditions. The central transect is chosen at the northern side of the basin, as this is located downstream of the eddy formation region.

The density structure is plotted as a function of the number of z layers and depth. As mentioned in Section 2.1, there are 40 layers with varying depths, at the surface the z layer is 20m, and at the bottom it is 200 m. Five density classes are defined ranging from $\rho = 28.5 kg/m^3$ to $\rho = 27.63 kg/m^3$, which corresponds to a temperature range from 2.5 to 7.5 degrees, with intervals of 1 degree. In each layer the difference in BC transport per density class, per segment is plotted. Thus, the first segment from inflow to the central transect has the goal to see how the water changes in depth and density space due to the eddy field. The second segment from central transect to outflow has almost no interaction with the eddies anymore but flows through the area with the largest winter surface heat loss. Thus, the impact of winter heat loss on overturning is investigated in this segment. It could be possible that the MLD near the western BC can reach into the BC directly, and can therefore directly export the convected water, as suggested by (Georgiou et al., 2020).

The red transects of Figure 2.4 are located inside the BC. It has been chosen to use a depth limit of 3000 m at the inflow and outflow, and 2600 m at the central transect. This difference in depth limit is chosen to have approximately equal volumes of water through each segment. Equal mass transport can only be approximated by taking the time-average of an entire year. The downside of a depth limit is that the bottom of the basin is not reached in the central transect while these are reached in the in- and outflow transects. Therefore, when the segments are analysed, a small discrepancy in the bottom two layers is found. Additionally, when computing the transport through the transects, only the velocity in the downstream direction is taken into account, to filter out a possible return current, and therefore only focus on the mass transport in the downstream direction.

Finally, when the studies into the dynamics on yearly timescales are finished, the effect on the dynamics on seasonal timescale are studied in Chapter 5. This is achieved, by studying how the BC transport changes per vertical layer, between the inflow and central transect. This is achieved by researching the mean difference of BC transport per vertical layer, for all the winter months (February and March) and all the summer months (August and September). These months are chosen, as the horizontal stratification in these months is respectively the strongest and weakest. Additionally, the total mass transport through this segment per month is plotted to see if the seasonality has a direct effect on BC export, or if it has a lagged response.

Then the results of the scenarios are interpreted and discussed in Chapter 6. The results can then be compared to observations and measurements, with the goal the qualitatively compare them, to better understand the dynamics of the Labrador Sea, and possibly improve the location and timing of the measurements.

3 | Results of consecutive strong winters

In this chapter, the results of the varying time series runs are presented. The structure of this chapter follows the methodology and starts off by comparing the relevant runs (to each other) by looking at the mean basin temperature (Section 3.1). Next, both the EKE and MLD of run 3yrDoubleHL is studied in detail (Section 3.2), runs 1yrDoubleHL and 5yrDoubleHL are qualitatively studied, compared to the 3yrDoubleHL run. Then a transect through the convection area of run 3yrDoubleHL is taken to study in detail how the density profile and velocities change every year (Section 3.3). Finally, the impact of winter heat loss on the overturning in the Labrador Sea is analysed, by looking into the difference in BC transport per vertical layer and density class (Section 3.4.

3.1 Mean basin temperature

In Figure 3.1 the basin mean temperature of REFG, REF, 1yrDoubleHL, 3yrDoubleHL and 5 yrDoubleHL are plotted over the simulation period. As discussed in Section 2.2 all runs use the 10th year of the reference run of (Georgiou et al., 2020) as the initial state. The black dotted line for REFG shows that for this simulation the equilibrium is reached in the 10th year, where the seasonal fluctuations stay around a constant temperature from year 10 to 20. The black line shows REF, in this run the Laplacian viscosity and diffusivity are changed, starting in the 10th year. In REF the surface heat flux is the same as in an average year and is equal to the one in REFG. With the change of the Laplacian viscosity and diffusivity, the basin tends to a new equilibrium. This trend is a constant reducing mean temperature of the basin. When comparing the different runs with the REF run this trend is taken into consideration.

The 3yrDoubleHL run is shown in blue in Figure 3.1. It is identical to the first 22 months of the 1yrDoubleHL. However, this run has two more strong winters in years 12 and 13. In the 5 years after the extreme heat loss events, the basin mean temperature stays almost constant, indicating that this temperature is the new equilibrium of the basin mean temperature, at approximately 3.4 °C. In the same figure the basin mean temperature of the 1yrDoubleHL run is shown in pink. In the 5 years after the additional surface heat loss event, the basin mean temperature continues to decrease toward the new basin equilibrium. The 5yrDoubleHL run is shown in red and has in total 5 strong winters from years 11 to year 15. In the 5 years after the extreme heat loss events, the basin mean temperature trends higher toward the new basin equilibrium.

It is clear from the basin mean temperature trend that a single strong winter already has a large impact on the mean basin temperature. Especially multiple strong winters reduce the temperature significantly. This suggests that the cooled water from the wintertime heat loss is not immediately flushed out during the summer months or by the BC. Therefore cold water likely remains in the basin to be further affected in the following winter. This should be able to be verified by looking at the MLD and transect of the basin in Sections 3.2 and 3.3.

Additionally, the basin tends to a new equilibrium. The REFG equilibrium is used as starting point of the runs, however due to the change in Laplacian viscosity and diffusivity, the basin tends to a lower basin mean temperature equilibrium.

For reference, in REF the average reduction of mean basin temperature is 0.016 °C per year. During years with an additional surface heat loss, the mean basin temperature is reduced on average by 0.065 °C, where the reduction in temperature is largest when the basin is furthest from the new basin equilibrium.

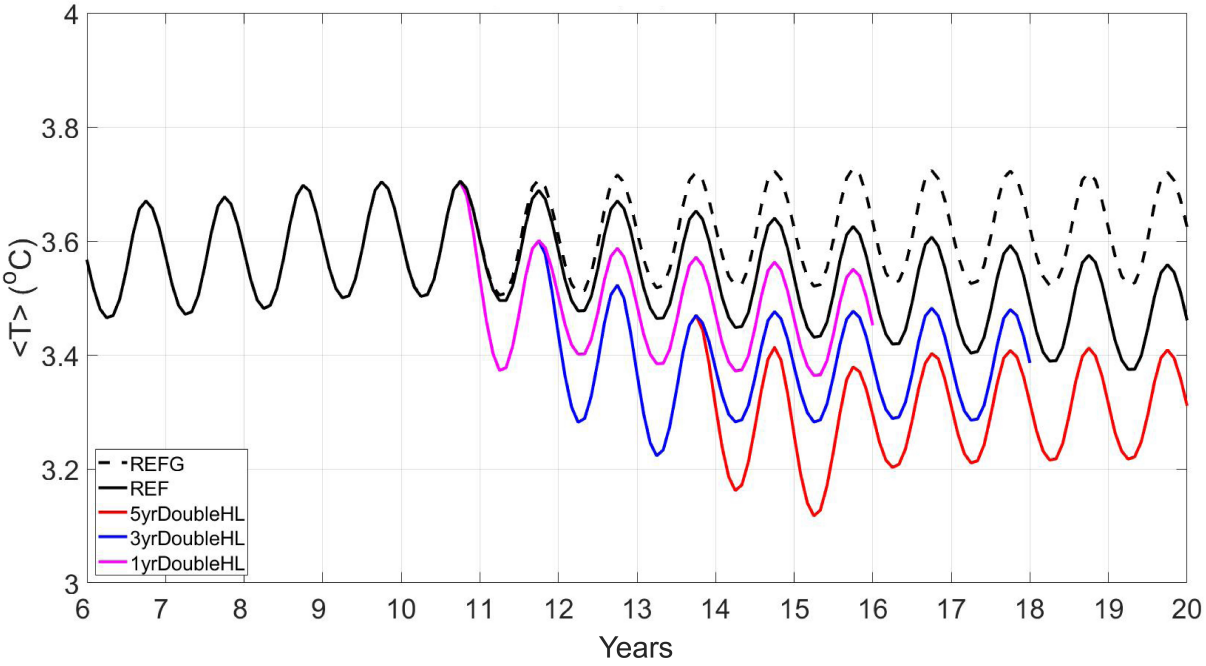

Figure 3.1: Basin mean temperature (in °C, on the y-axis) of the consecutive strong winter runs. The years are plotted on the x-axis and start from year 6 to year 20. The runs REF in solid black, 5yrDoubleHL in red, 3yrDoubleHL in blue and 1yrDoubleHL in pink, have as starting point year 10 of REFG (dashed black).

3.2 Eddy kinetic energy and mixed layer depth

The analysis of the eddy kinetic energy (EKE) for this section is based on run 3yrDoubleHL. This run is chosen as it is the moderate run of the consecutive winter runs. All the plots in this subsection are based of this run. First, the EKE and MLD per year of 3yrDoubleHL are studied in Figure 3.2. Then in Figure 3.3 the difference in EKE and MLD between 3yrDoubleHL and REF is studied to quantify how the system behaves in relation to an average heat loss. The results of the runs 1yrDoubleHL and 5yrDoubleHL are qualitatively treated and discussed at the end of the section.

In Figure 3.2 the mean EKE and MLD of February and March of 3yrDoubleHL are plotted per year. In Figures 3.2b-d, the surface heat flux is doubled in comparison to the other years. In the first year, the MLD has a maximum of around 1650 m and is focused in the interior. During these strong winter years, the MLD increases almost up to the maximum of the basin depth of 3000 m. These maxima are centered in the interior, near the area with the most heat loss, see Figure 2.1. However the MLD does not only increase in the area with the most intense surface heat loss, but also increases far outside this region, towards the south and east. In the years after the 3 years of additional surface heat loss (Figure 3.2e-h), the maximum MLD exceeds depths of 2000 m and is again centered in the interior.

In shading in Figure 3.2b-d is seen how the EKE changes due to additional surface heat loss. In the BC near Greenland this increase is the most noticeable. Where it can be observed that the increase in eddy activity is forced through the BC, and not into the interior. The eddies are redirected along the area of increased MLD in all years. In Figures 3.2e-h, an average heat loss is applied and the EKE decreases in intensity and also in area. In all these years both the EKE and MLD stay relatively constant. The runs 1yrDoubleHL and 5yrDoubleHL have similar results as 3yrDoubleHL, it is observed that the MLD increases in the interior and the EKE increases in the eastern BC. 1yrDoubleHL and 5yrDoubleHL do not show any additional insights, nonetheless they can be seen in the Appendix in Figure A.3 and Figure A.4.

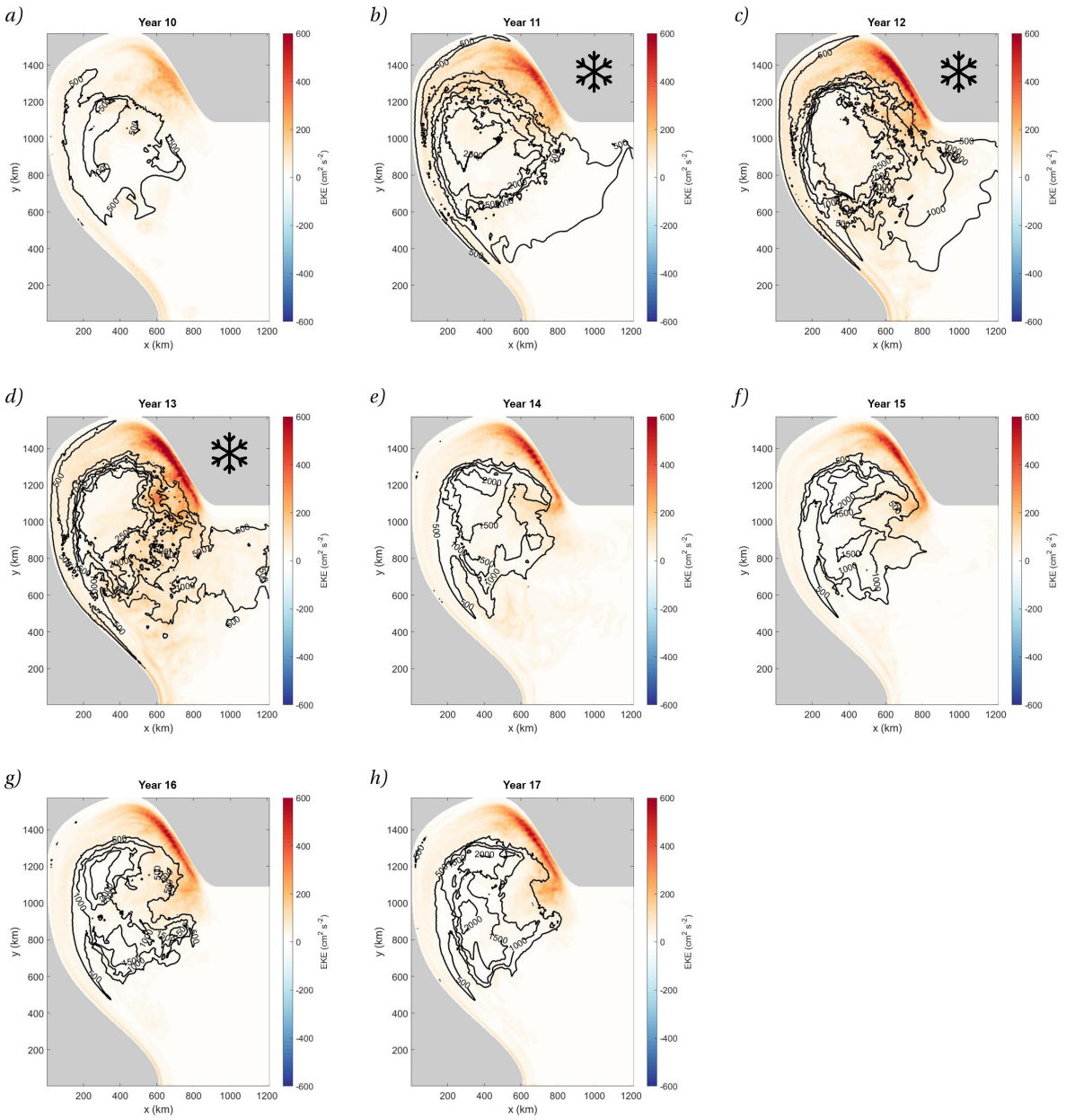

Figure 3.2: Mean EKE (shading) and MLD (contours) per year, based on the months February and March for run 3yrDoubleHL. The MLD is plotted with contour lines in meters, with intervals of 500m. The EKE is shaded and expressed in cm^2/s^2. The surface heat loss is double the average surface heat loss in the years 11, 12 and 13, depicted by frost signs.

In Figure 3.3 the difference in EKE and MLD between 3yrDoubleHL and REF is studied. It should be noted that REF is not in basin equilibrium and has a decreasing mean basin temperature trend. Resulting in a MLD exceeding 2000 m in the first year, and increasing every year up to, and exceeding 2500 m in the last year. Additionally as the MLD increases in the interior, the EKE increases in the eastern BC. This is shown in the Appendix in Figure A.2.

In Figure 3.3a the forcing is the same in both runs and therefore both MLD and EKE are equal. In Figure 3.3b-d additional surface heat loss is applied and it is seen how this significantly impacts both EKE and MLD. The MLD difference with REF in these years is on average 1000 m in the first strong winter, and up to 2000 m in the third strong winter. Additionally the increase in EKE, is most pronounced in the BC, especially near Greenland. In Figure 3.3e-h the EKE remains larger than in the REF in the BC, but decreases in the interior. Finally the only significant difference in MLD in the years after the extra heat loss, is found in Figure 3.3e. Where locally the MLD is still up to 1000 m deeper than in REF. In Figure 3.3f-h only small areas in the interior still have increased MLD's.

The reason that the EKE increases mainly in the eastern BC, is due to the increased MLD in the interior. As the interior is now much colder than the BC, an increased horizontal density gradient is formed. Thus leading to an increase in velocity in the BC, as seen in the thermal wind balance, see Equation 1.1. As the velocity increases, the BC becomes more unstable and more eddies are shed into the interior, thus causing an increase in EKE. These eddies from the BC do not easily shed into the interior anymore, due to a steep front of dense water caused by the increased MLD near the eastern BC, therefore the eddies tend to be less perpendicular to the BC and are therefore more downstream directed. Therefore, the increase of EKE is focused in the BC and less into the interior. This is also observed in Figures 3.3e-h (in the years after the strong winters), where areas of light blue indicate a decrease of EKE compared to REF. Thus it suggests that the amount of eddies decreases in these regions, as seen in Figure 3.2e-h, these regions coincide with a locally large MLD. The persistence of increased EKE in the years after the additional surface heat loss can also be attributed to the thermal wind balance. The interior is colder than in REF, which can also be observed in Figure 3.1, thus the horizontal density gradient is therefore greater in 3yrDoubleHL than in REF. Thus, the velocity in the BC is higher because the horizontal density is greater, causing the BC to be less stable and causing an increase in the amount of eddies shedding from the BC, therefore causing the increase in EKE compared to REF.

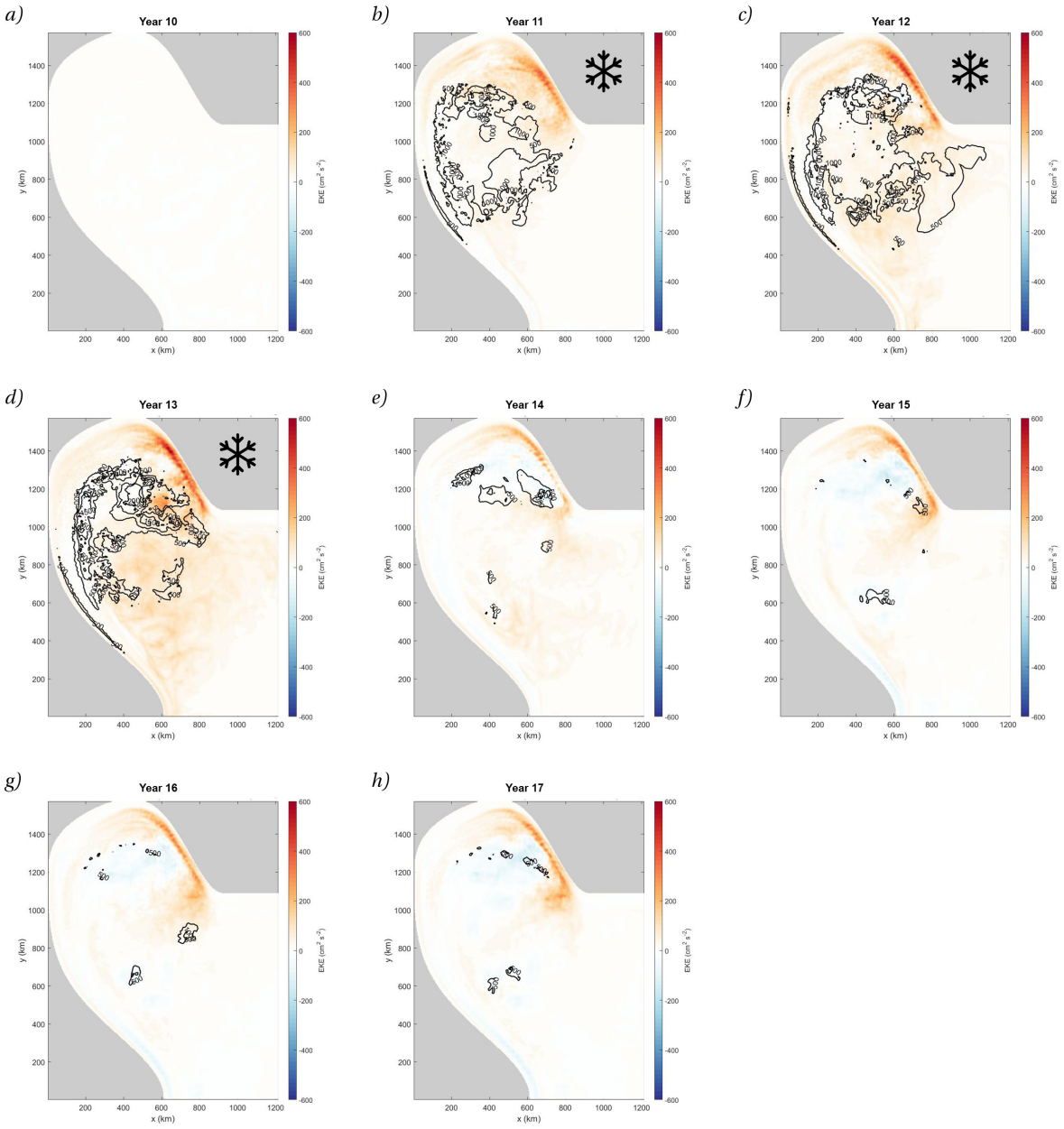

Figure 3.3: The mean EKE (shading) and MLD (contours) difference for each model year 3yrDoubleHL and REF from year 10 to year 17. From each 3yrDoubleHL the associated REF year is subtracted. is In panel b-d (year 11, 12 and 13) the heat loss is doubled with respect to the average heat loss, depicted by frost signs. The EKE and MLD values are averaged over the months February and March, as in Figure 3.2.

3.3 Properties across the basin

In this section it is investigated what the properties are of 3yrDoubleHL of the transect through the basin, defined in Figure 2.4. In this section is studied how the interior reacts to strong winters, by looking into the changes in density structure and velocity changes. The density structure is expressed by isopycnals, defined as white lines, with contour intervals of $\sigma = 0.01 kg/m^3$. The velocities are shown in black lines, indicating a positive velocity, perpendicular to the transect. The dashed black line, indicates a negative perpendicular to the transect. The mean temperature is indicated in shading. The vertical red lines indicate the limits of the BC based on the barotropic streamfunction, which is fixed at 18 Sv. In Figure 3.4a-h an overview of the transect of the 3yrDoubleHL run for years 10 to year 17 is shown. It should be noted that although the water between $\sigma = 28.35$ and $\sigma = 28.4 kg/m^3$ is in direct contact with the surface, this is not equal to the mixed layer depth. The mixed layer depth is defined as a difference of $\sigma = 0.005 kg/m^3$, with respect to the surface.

First the development of the isopycnals is discussed, they are essentially the same as the temperature shading, as salinity is neglected. However by depicting them as isopycnals, the structure of the densities is easier to study. The initial state (year 10) is seen in the Figure 3.4a, which has an isopycnal structure defined by horizontal isopycnals. The isopycnal contour lines range from $\sigma = 28.35 kg/m^3$ to $\sigma = 28.5 kg/m^3$, corresponding to a temperature range of 3.4 °C to 2.5 °C. The isopycnals in the BC are not illustrated, as the focus in this section is on the development of the density structure in the interior, and at the BC limit. In Figure 3.4b-d, due to the strong winters the density structure is defined by vertical isopycnals. The columns of water in the interior inbetween the vertical isopycnals extend from the surface to the bottom of the basin. This strong vertical isopycnal structure to the bottom of the basin, forms after two consecutive strong winters. In the bottom half of the basin in the interior, the horizontal isopycnal structure is recovered in the first year after the strong winters, as seen in Figure 3.4e. In the subsequent years (Figure 3.4f-h), the system remains approximately constant with a horizontal isopycnal structure in the bottom half of the basin. The upper half of the basin is defined by a vertical isopycnal structure.

In the 1yrDoubleHL (Figure A.3) and 5yrDoubleHL (Figure A.4) runs similar density structure development is observed. However, the density structure of the upper layers in the years after the additional surface heat loss varies. The vertical isopycnal structure at the upper layers in the interior of 1yrDoubleHL remain on average up to depths of 2000 m. The vertical isopycnal structure at the upper layers in the interior of 3yrDoubleHL remain on average up to depths of 1500 m, as can be seen in Figure 3.4e-h. The vertical isopycnal structure at the upper layers in the interior of 5yrDoubleHL remain on average up to depths of 1000 m. This difference between the runs, is due to the amount of consecutive strong winters, and therefore the amount of dense convected water. The convected water is not flushed out during the summer months, and therefore a gradual increase of convected water is observed in Figure 3.4b-d. Therefore due to 5 consecutive strong winters the amount of accumulated convected water is larger than the amount of accumulated convected water of one strong winter. Thus, the larger the volume of dense water is present at the bottom, the shallower the vertical density structure is in the upper layers in the years after the strong winters.

It is observed that the basin is not able to flush out the convected water of the strong winters immediately. However in Figure 3.4e-h can be observed that the densest water from isopycnal $\sigma = 28.44 kg/m^3$ decreases in volume throughout the years. The water from this isopycnal barely reaches into the eastern and western BC and is therefore likely not able to export all of its water through the BC. Therefore it suggests that the water is exported near the bottom of the basin due to a pressure difference between the middle of the interior and outside the interior. As the deep convected water at these depths is heavier than water outside the interior at these depths, thus forming a baroclinic flow, exporting the deep convected water out of the interior.

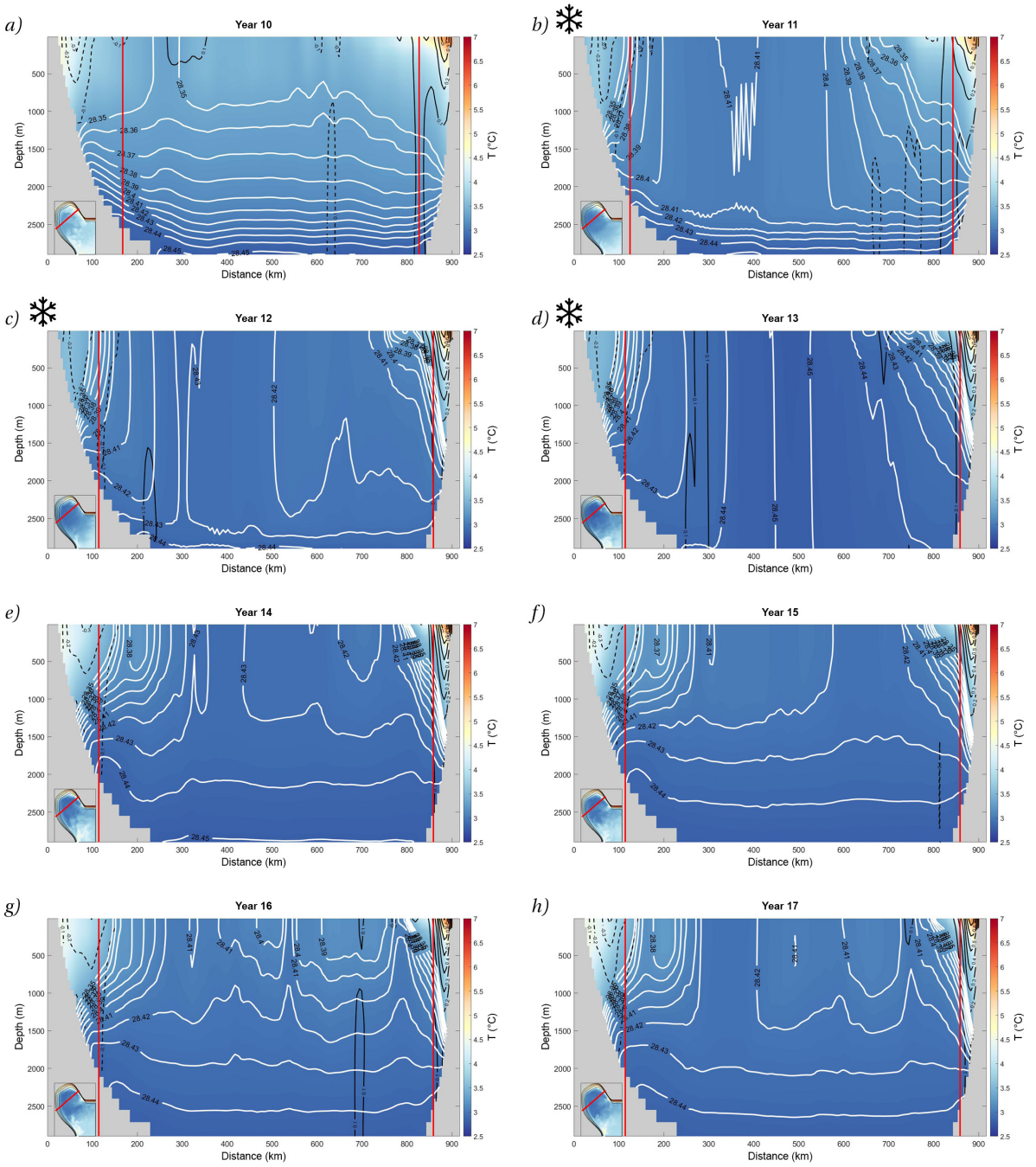

Figure 3.4: a-h) Transect through the convection area, as indicated in the inset in the bottom left corners, by the red line. The mean temperature of the months February and March of run 3yrDoubleHL is plotted for every year and indicated in shading (in °C). The white contour lines define the isopycnals, with $\sigma = \rho - 1000 kg/m^3$. The black contour lines indicate the positive velocities and the dashed black lines are the negative velocities, with an interval of 0.1 cm/s. The vertical red lines indicate the limits of the BC based on the barotropic streamfunction, which is fixed at 18 Sv. The years with strong winters are depicted by frost signs.

Now the structure of the isopycnals near the eastern and western BC and through the BC limit are studied. A relatively vertical isopycnal structure is formed at both sides of the basin crossing into BC. This vertical structure practically remains constant in the years after the additional surface heat losses (more so on the eastern side). In Figure 3.5 the eastern BC is enhanced of year 16 of 3yrDoubleHL as an example, to study in more detail what the transect in the eastern BC looks like. The isopycnals shown in this figure correspond to the densities ranging from $\sigma = 28.14 kg/m^3$ to $\sigma = 28.42 kg/m^3$. The isopycnals inside the

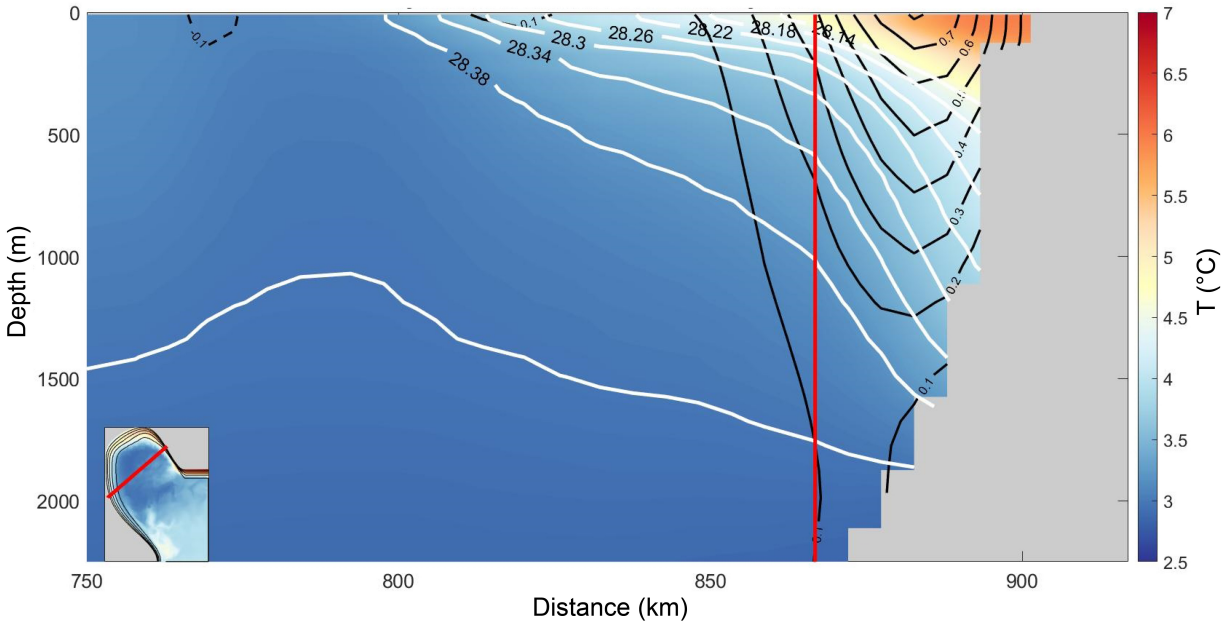

Figure 3.5: An example of the isopycnal structure in the eastern BC in the winter months (February - March of year 16). Isopycnals range from $\sigma = 28.42 kg/m^3$ to $\sigma = 28.14 kg/m^3$, with white contour intervals of $\sigma = 0.04 kg/m^3$. The velocity is described by black contour lines, ranging from 0.1 cm/s to 0.8 cm/s. The red line, indicates the BC limit, based on a transport limit of 18 Sv.

BC are almost vertical, whereas in the interior they are more horizontal. This structure is also found in all the other years and runs, regardless of additional surface heat loss. This indicates that the eddies at the surface try to shed into the interior, making the isopycnal structure more horizontal.

Finally the focus is on the velocity profiles, depicted as black contour lines in Figure 3.4 and Figure 3.5. The velocities are perpendicular to the transect of the basin. In the western BC the velocity is negative as it flows southwards. In the eastern BC the velocity is positive as it flows northwards. In Figure 3.4a the velocities at the surface exceed 0.3 cm/s on the western side, and in the eastern side exceed 0.4 cm/s. From Figure 3.4b-h the velocities on the surface increase in the eastern side up to 0.7 cm/s. In the western boundary the velocities stay approximately the same. The velocity in the eastern BC increases throughout the entire depth of the BC, up to 0.1 cm/s at the bottom. Due to this increase in velocity over the entire depth, the eastern BC limit changes, depicted as red lines in Figure 3.4. As the velocity increases, the BC limit narrows.

The increase in velocity in the eastern BC is matched by the results from Section 3.2, which show an increase of EKE in this region. These transects confirm that the EKE has difficulty to shed into the interior due to the front near the eastern BC. And therefore the eddies are directed more towards the downstream BC direction, thus increasing the velocity in this region. Whereas in the western BC there is no influence of eddies, and therefore has no increase in velocity in this part of the transect.

3.4 BC transport per vertical layer and density class

In previous sections is described how the different interactions change due to (consecutive) strong winters. In this section the corresponding change in distribution of BC transport in the vertical and by density class is analyzed to assess changes in the BC structure indicative of overturning and eddy exchange. This is done by looking at the change in transport in two segments of the BC, as defined in Section 2.3.d. A distinction is made between the years with additional surface heat loss (years 11,12 and 13) and the years afterwards (years 14,15 and 16). The eastern segment through which the change is studied, is the segment from the inflow to the central transect of the BC (downstream of the topographic narrowing). The second segment is between the central transect of the BC and the outflow (red lines in Figure 2.4).

First the amount of total transported water (in Sv) through each section is shown in Table 3.1, to see if the volume through each transect is (approximately) equal. The total transport through each section is summed and averaged per year. Additionally, two more averages are taken of the additional surface heat loss years and of the subsequent years depicted in bold. It shows a large year to year difference between each transect (approximately 3 Sv), but when three years are averaged the difference between each transect is in the order of 1 Sv. Therefore this section uses the three year averaged BC transport to further study the BC transport per segment.

From studying the three year averaged BC transports (Table 3.1), it strikes the most that the total transport through the outflow is significantly reduced in the years after the additional surface heat loss (19.6 Sv), compared to years with additional surface heat loss (21.1 Sv) and compared to the transport through the central transect (22.7 Sv). This difference in transport in the western segment is significant and should be considered when making the BC transport comparisons. Additionally, the transport in the central transect increases in all years, compared to the inflow. This increase in transport is likely due to the increase in velocity in the eastern BC, which is shown in Section 3.3.

Table 3.1: The net transport (in Sv) per year, through the inflow, central and outflow transects from 3yrDoubleHL. Highlighted in bold are the years with additional surface heat loss. Note that the transports are negative, as the flow from East to West are in the negative x direction.

Year	Sum inflow	Sum central	Sum outflow
10	-20.3	-14.1	-22.0
11	**-20.4**	**-18.3**	**-21.0**
12	**-20.9**	**-23.9**	**-21.3**
13	**-22.4**	**-24.2**	**-21.0**
14	-21.8	-23.4	-19.7
15	-21.3	-23.0	-19.4
16	-21.9	-21.8	-19.5
17	-21.4	-21.5	-19.5
Mean yr 11 - 13	**-21.2**	**-22.1**	**-21.1**
Mean yr 14 - 16	-21.7	-22.7	-19.6

Figure 3.6a shows the difference in transport of water per density class, between the inflow and central transect, averaged over the years with additional surface heat loss (year 11, 12, 13). A large increase of the densest water, as shown in blue, is found (in interval $\sigma = 28.33 - 28.5 kg/m^3$), from layer 22 (1000 m depth) to layer 37 (2475 m depth). The water in the intervals from $\sigma = 28.33 kg/m^3$ and lighter mostly decline through this segment of the BC. Specifically the warmer water from interval $\sigma = 27.80 - 27.98 kg/m^3$ (purple), and $\sigma = 27.63 - 27.80 kg/m^3$ (green), decrease in the upper 6 layers (150 m depth).

In contrast Figure 3.6b shows the difference in transport of water per density class, between the central transect and outflow, averaged over the years with additional surface heat loss (year 11, 12, 13). The densest water interval, shown in blue, increases significantly from the layer 5 up to layer 27 (100 m to 1375 m depth). Additionally the water from interval $\sigma = 28.15 - 28.33 kg/m^3$ (dark orange), increases in the top 9 layers (300 m depth). But a larger volume of water from the dark orange interval decreases from layer 11 to layer 27 (400 to 1375 m depth). Furthermore a large volume of water from interval $\sigma = 27.98 - 28.15 kg/m^3$ (yellow), decreases significantly from the surface layer to layer 15 (600 m depth). Finally the water from interval $\sigma = 27.80 - 27.98 kg/m^3$ (purple) decreases in the upper 9 layers (300 m depth).

The differences in transport of water per density class during the strong winter years can be explained in relation to the interactions in the basin. The first segment between inflow and central transect a large increase of densest water is observed and a large decrease in buoyant water. This indicates that due to the eddy exchange there is strong overturning in the eastern BC segment. It is theorised in previous chapters (Section 3.2) that it is unlikely this exchange happens during the winter, due to the strong wintertime front near the eastern BC. Therefore, this suggests the eddy exchange takes place in other months. This exchange most likely happens in the summer as the interior then restratifies. The overturning as observed in the second segment is also an expected outcome. As the water in the western BC flows through the area with largest heat loss it therefore loses buoyancy to the atmosphere. Thus results in overturning from the lighter density classes into dense water.

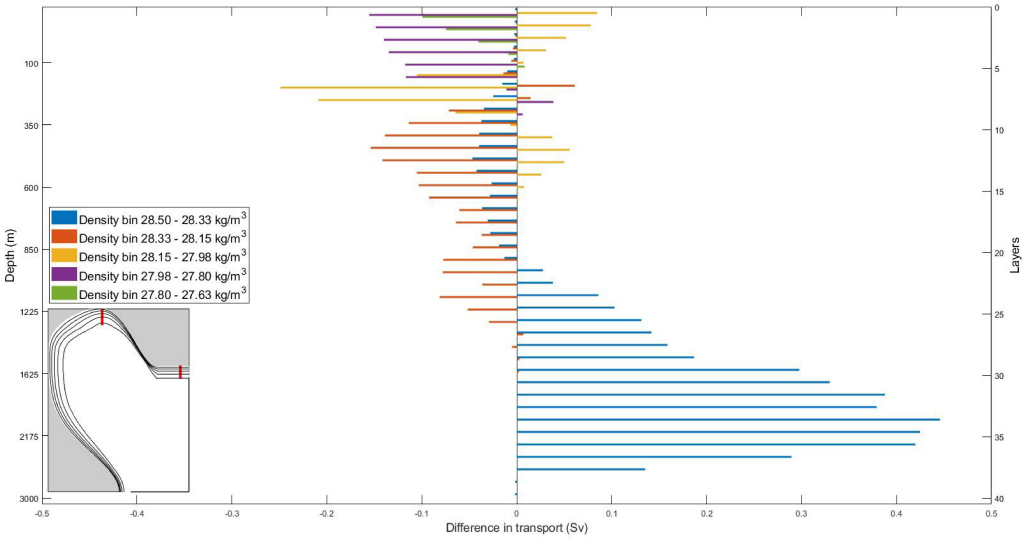

(a)

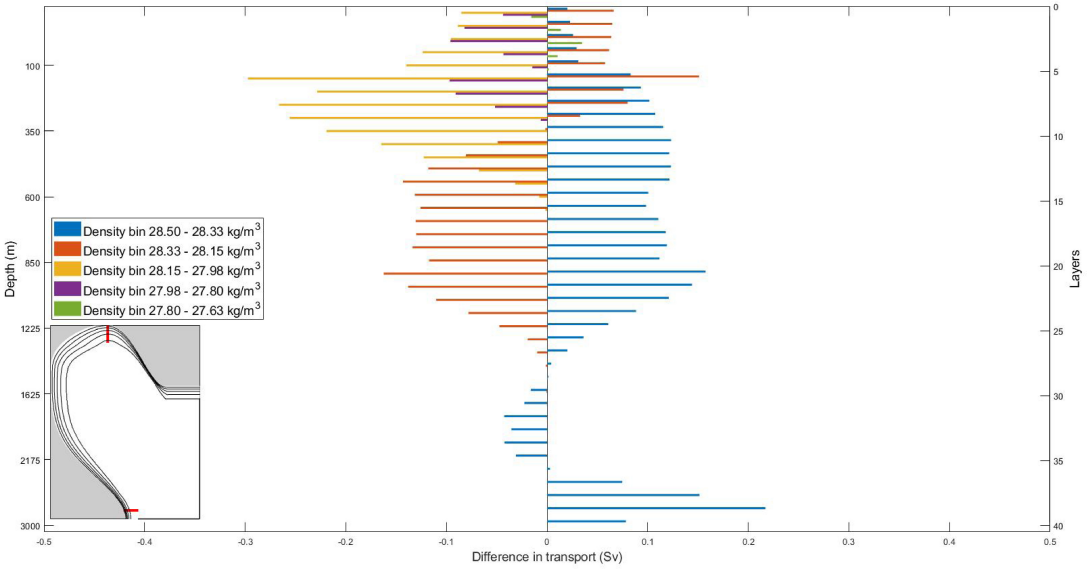

(b)

Figure 3.6: The difference in BC transport per segment of 3yrDoubleHL. Plotted as the mean of the years with additional surface heat loss (year 11,12,13). The left y-axis is defined as the depth (in m) the right y-axis is defined as the z layers. A positive (negative) difference in transport indicates that the volume of transported water from the density class increases (decreases). a) The segment in the BC between the inflow and central transect. b) The segment in the BC between the central transect and the outflow, indicated in the subplot in the bottom left corner. The density class of blue is $\sigma = 28.33 - 28.5 kg/m^3$, dark orange is $\sigma = 28.15 - 28.33 kg/m^3$, yellow is $\sigma = 27.98 - 28.15 kg/m^3$, purple is $\sigma = 27.80 - 27.98 kg/m^3$ and green is $\sigma = 27.63 - 27.80 kg/m^3$.

Next is discussed the difference in transport of water per density class, between the inflow and central transect, averaged over the years with average heat loss (year 14, 15, 16). In Figure 3.7a a similar pattern as in Figure 3.6a is found. Approximately the same amount of dense water from interval $\sigma = 28.33 - 28.5 kg/m^3$ (blue), is added from layer 22 to layer 37 (1000 m to 2475 m depth). However, a larger portion of the water from this interval is removed from layer 6 to layer 23 (150 m to 1075 m depth), compared to the removal seen in these layers in Figure 3.7. The fact that similar patterns are found in the years after additional surface heat loss is notable, it implies that the processes that are forced by the strong winters continue in the years afterwards.

Finally in Figure 3.7b is the difference in transport of water per density class, between the central transect and outflow, averaged over the years with average heat loss (year 14, 15, 16). The changes in transport are very different than the years with additional surface heat loss (Figure 3.6b). The large increase of the densest water from layer 5 to layer 27 (100 m to 1375 m) is not present anymore (Figure 3.6b). Instead a large increase of water from interval $\sigma = 28.15 - 28.33 kg/m^3$ (dark orange), is present from the surface layer up to layer 12 (450 m depth) and a (relatively smaller) decrease is found in layer 11 up to 26 (400 m to 1300 m depth). Furthermore a large decrease is found of the densest water interval $\sigma = 28.33 - 28.5 kg/m^3$ (blue) from layer 16 to layer 37 (650 m to 2475 m depth). The previously seen overturning in density space due to the cold winter in Figure 3.6b is not present anymore in the years afterwards. Now it is mainly characterised by a large increase of water in the dark orange interval near the surface. It can be speculated that the water from the yellow interval is convected due to average winter surface heat loss, and thus results in the increase of dark orange water interval, however it is odd that this occurs in the upper layers. With more certainty can be speculated that the basin is sensitive to the surface heat loss and therefore has a large impact on the BC transport. This is additionally seen in Table 3.1, which shows how variable the year to year BC transport can be, and even the three year averaged western segment transport still has a difference of 3 Sv.

Similar behaviour as discussed in this section is found in the runs 1yrDoubleHL and 5yrDoubleHL (but not shown).

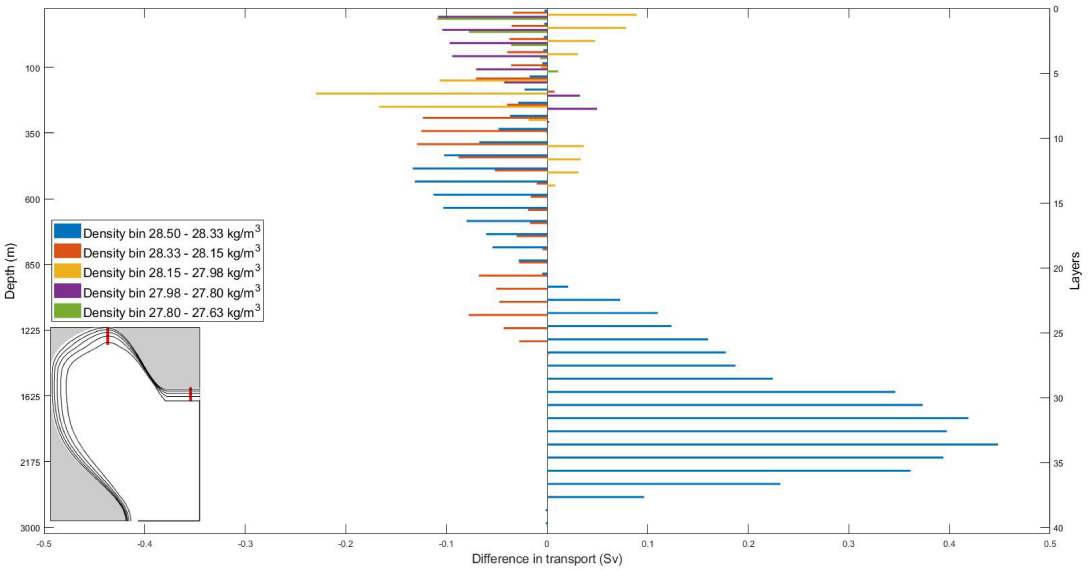

(a)

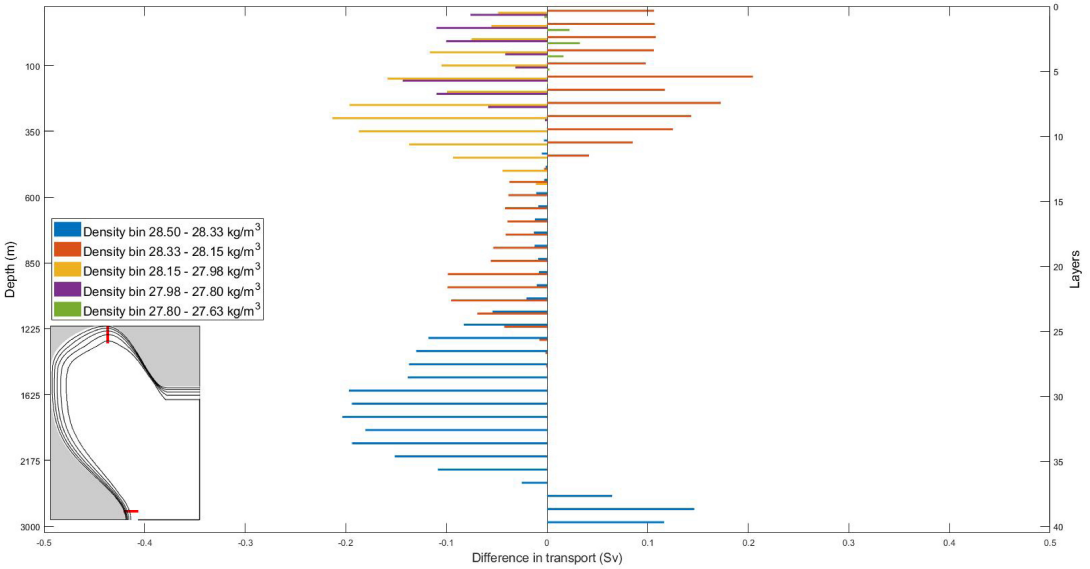

(b)

Figure 3.7: The same as Figure 3.6, but for the years after the additional surface heat loss (years 15,16,17).

4 | Varying heat loss intensity runs

In this chapter the results of the varying heat loss intensity runs are presented. The structure of this chapter follows the methodology and starts of by comparing the relevant runs (to each other) by looking at the mean basin temperature (Section 4.1. Next, the EKE and MLD of run 1yrTripleHL is studied in detail and compared to 1yrDoubleHL and REF (Section 4.2). Then a transect through the convection area of run 1yrTripleHL is taken to study in detail how the density profile and velocities change every year (Section 4.3). Finally the impact of winter heat loss on the overturning in the Labrador Sea is analysed, by looking into the difference in BC transport per vertical layer and density class (Section 4.4).

4.1 Mean basin temperature

In Figure 4.1 the basin mean temperature of REFG, REF, 1yrDoubleHL and 1yrTripleHL is plotted over the simulation period. This Figure has the same properties as Figure 3.1, but with the runs of the intensity based scenario. In green the 1yrTripleHL run is shown, and in pink is the 1yrDoubleHL shown, which is previously discussed in the Chapter 3. Due to the extreme winter of the 1yrTripleHL run the temperature decreases by 0.236 degrees compared to REF. In comparison, the decrease in temperature in 1yrDoubleHL run during the first winter is 0.112 °C compared to REF. In the 5 years after the additional surface heat loss event the basin mean temperature of 1yrDoubleHL and 1yrTripleHL continue to lower. In Figure 3.1 is established they tend to the new mean basin equilibrium temperature of 3.4 °C.

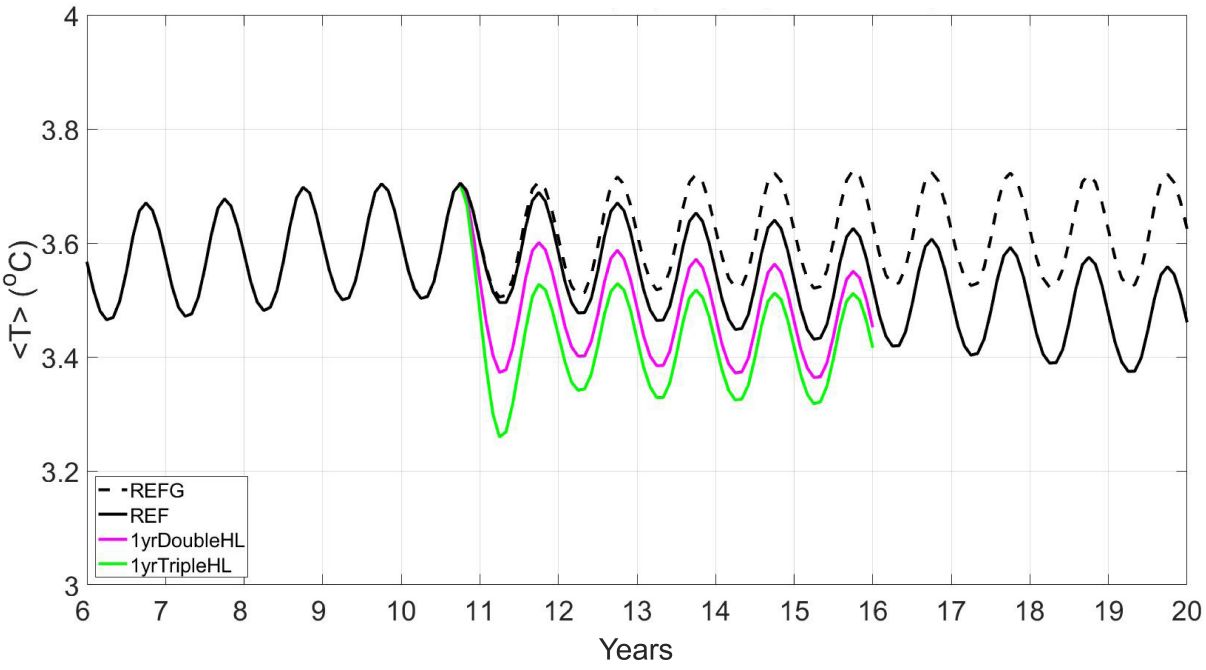

Figure 4.1: Basin mean temperature (in °C, on y-axis) of the varying heat loss intensity runs. The years are plotted on the x-axis and start from year 6 to year 20. The runs REF in solid black, 1yrTripleHL in green and 1yrDoubleHL in pink, have as starting point year 10 of REF (dashed black).

4.2 Eddy kinetic energy and mixed layer depth

The analysis on the eddy kinetic energy for this section is based on run 1yrTripleHL. First the EKE and MLD per year of 1yrTripleHL is studied in Figure 4.2. Next in Figure 4.3 the difference in EKE and MLD between 1yrTripleHL and REF is studied to quantify how the system behaves in relation to an average heat loss. Then in Figure 4.4 the difference between 1yrDoubleHL and 1yrTripleHL are studied.

In Figure 4.2 the mean EKE and MLD of February and March of 1yrTripleHL are plotted per year. In Figure 4.2b, during the extreme winter, the MLD increases almost up to the maximum of the basin depth of 3000 m. The deepest MLD's are formed in the interior, near the area with the most heat loss, see Figure 2.1. However the MLD also deepens far outside this region, towards the south and east side of the interior and into the western BC (near Canada). In the years after the additional surface heat loss, the maximum MLD decreases to 2500 m and is confined in the interior.

The shading in Figure 4.2 shows how the EKE changes due to the additional surface heat loss. Especially in Figure 4.2b is seen how the EKE increases significantly in the eastern BC, due to the additional surface heat loss. Similar to the results in Section 3.2, the increase in eddy activity is forced along the area of increased MLD, and therefore tend to be less perpendicular to the BC and are more downstream directed. The eddies are forced to pass along the area of increased MLD in all years, as they are not able to shed through the strong front. In Figure 4.2c-f, when average heat loss is applied, the EKE decreases in intensity and also in area. From that year on, both the EKE and MLD stay relatively constant.

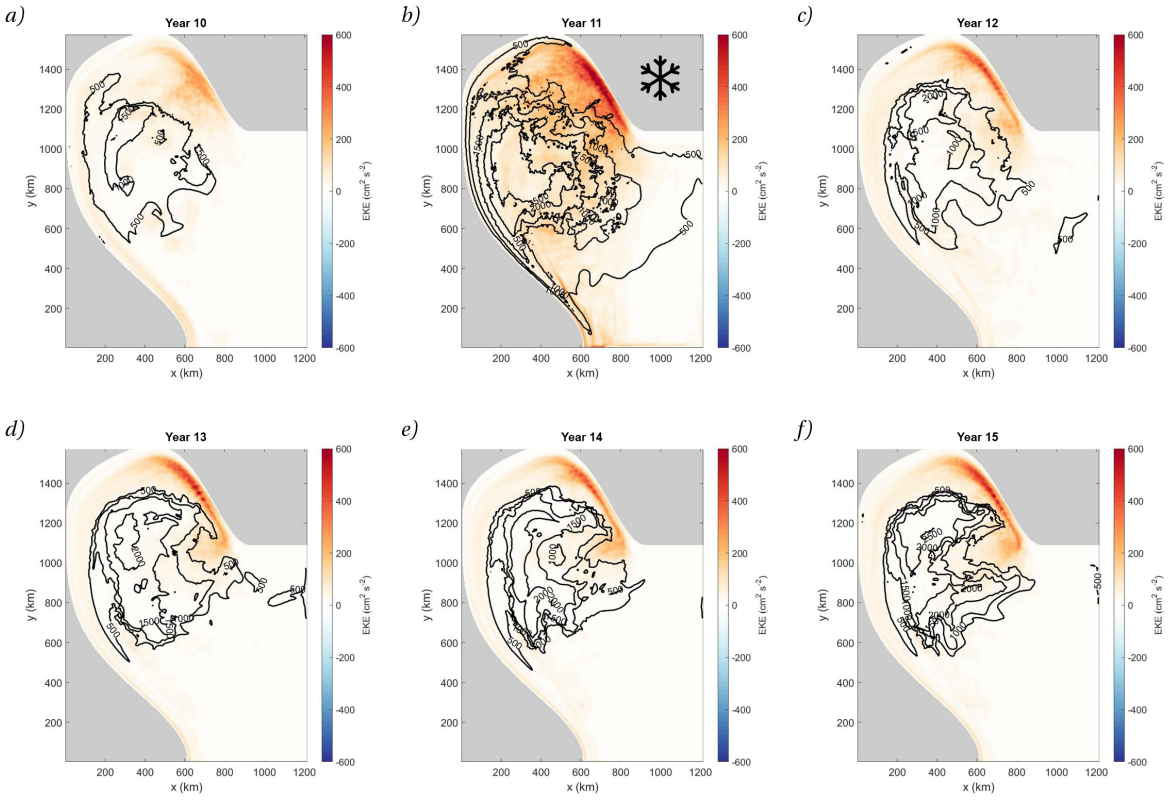

Figure 4.2: Mean EKE (shading) and MLD (contours) per year, based on the months February and March. The MLD is plotted with contour lines in meters, with intervals of 500m. The EKE is shaded and expressed in cm^2/s^2. In year 11 the surface heat loss is triple the average surface heat loss, depicted by a frost sign.

In Figure 4.3 the difference between EKE and MLD has been plotted for the 1yrTripleHL and REF run. In Figure 3.3a the forcing is equal and therefore both MLD and EKE are equal. In Figure 4.3b (year 11) is the additional surface heat loss applied, this results in a relative deepening of the MLD, focused in the western BC and the western side of the interior. Especially the MLD in the western BC is significantly deepened: in an average winter year the BC MLD is less than 500 meters in this region, and now exceeds 500 m to 1500 m locally. The EKE in the western BC increases significantly in this year as well relative to REF. In Figure 4.3c-f, when normal winter heat loss is applied, the MLD difference with REF exceeds 1000

m locally, but no pattern is observed. The EKE in the western BC increases up to 300 cm^2/s^2 and stays approximately constant throughout these years. Noticeably are the blue areas, indicating a decrease of eddies in the interior. Apparently the amount of eddies decreases in part of the interior. When comparing these areas with Figure 4.2c-f, these areas approximately coincide with local large areas of MLD, therefore reaffirming that the amount of eddies decrease in regions of increased MLD, as earlier suggested in Section 3.2.

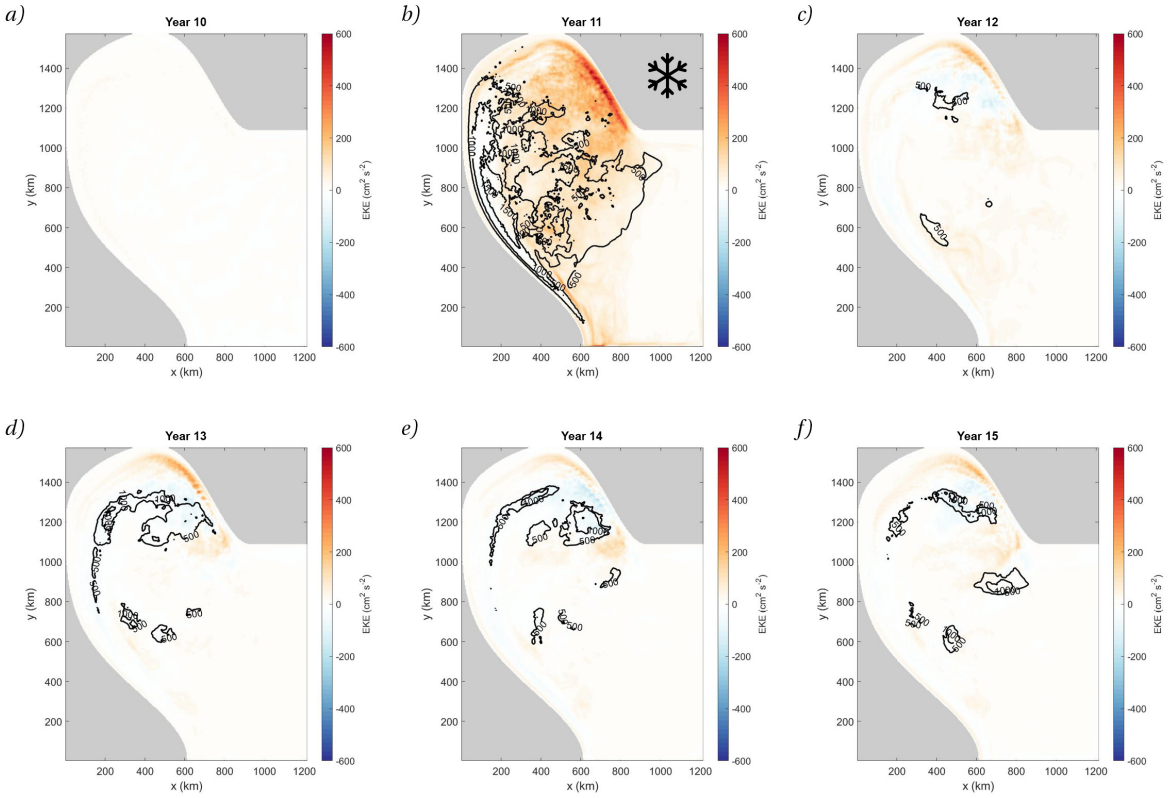

Figure 4.3: The mean EKE (shading) and MLD (contours) difference between 1yrTripleHL and REF from year 10 to year 15. In year 11 the surface heat loss is triple the average surface heat loss, depicted by a frost sign. The EKE and MLD values are averaged over the months February and March.

In Figure 4.4 the difference between EKE and MLD has been plotted for the 1yrTripleHL and 1yrDoubleHL runs. The most striking difference is that the MLD difference exceeds 1000 m in the year with additional surface heat loss, in the western BC (Figure 4.4b). In Figures 4.4c-f, minor differences in EKE and MLD are found, and especially no year to year trends are spotted. This indicates that an increased heat loss intensity does not have any long term effects, and only affects the western BC in the year with additional surface heat loss. Because the MLD increase is located mostly inside the western BC it is therefore likely that the convected water is directly exported through the BC, and therefore has no long term effect. The eastern BC is not affected significantly by the changes in heat loss intensity.

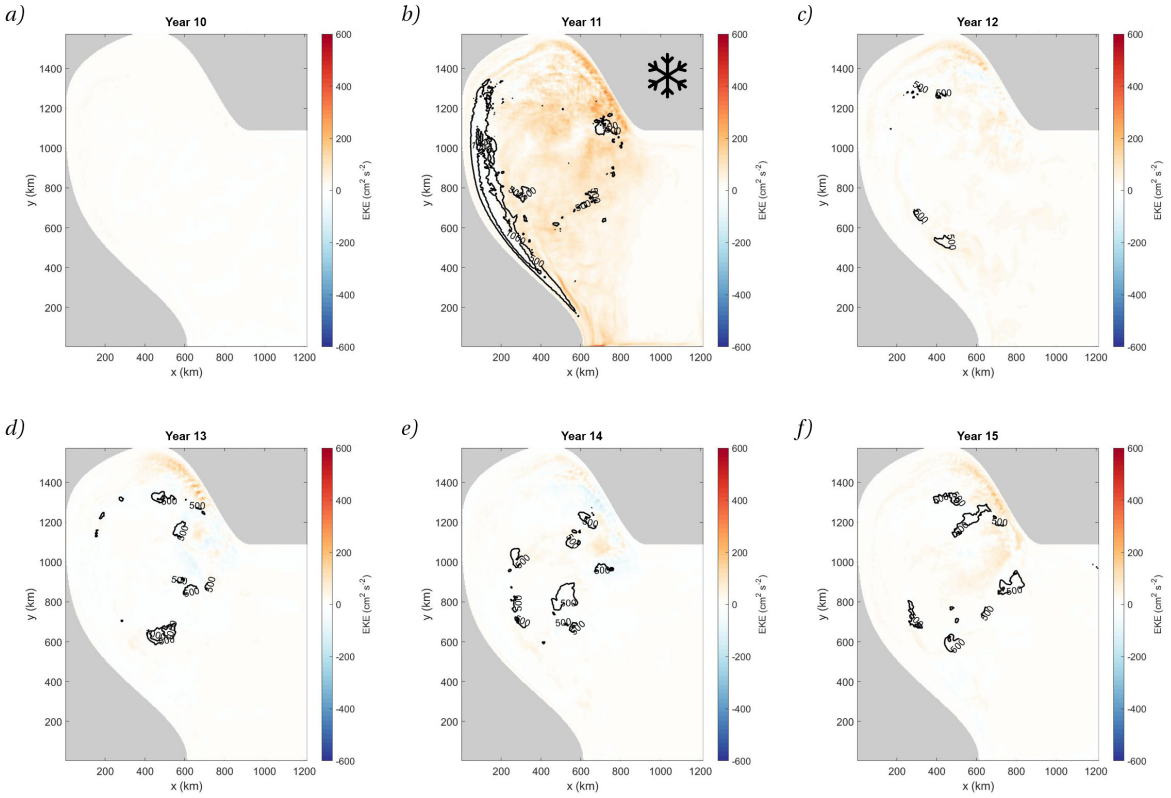

Figure 4.4: The mean EKE (shading) and MLD (contours) difference between 1yrTripleHL and 1yrDoubleHL from year 10 to year 15. In year 11 the surface heat loss is triple the average surface heat loss, depicted by a frost sign. The EKE and MLD values are averaged over the months February and March.

4.3 Properties across the basin

In this section it is investigated what the properties are of 1yrTripleHL of the transect through the basin, defined in Figure 2.4. In this section is studied how the interior reacts to an extreme winter, by looking into the changes in density structure and velocity changes, similarly to Section 3.3.

During the extra cold year, seen in Figure 4.5b, the isopycnals in and near the western BC become vertical. This is coincides with Figure 3.2b, which show a deep MLD in the western BC. In the years after the extreme winter (Figure 4.5c-f) 1yrTripleHL has a similar isopycnal structure as in the years after the strong winters of 3yrDoubleHL (Figure 3.4e-h). The vertical isopycnal structure in the upper layers in the interior after the extreme winter of 1yrTripleHL remains on average up to depths of 1750 (compared to an average depth of 2000 m in 1yrDoubleHL and 1500 m in 3yrDoubleHL). This is logical as a large amount of dense convected water remains near the bottom of the basin, and can therefore more easily be reached during a subsequent (average) winter. Just like in Figure 3.4e-h the densest water of Figure 4.5c-f ($\sigma = 28.44 kg/m^3$) is barely in contact with the eastern and western BC, but reduces in volume over the years. This reduction could therefore be attributed to the baroclinic pressure difference as suggested in Section 3.3. Or alternatively the convected water could be in contact with the western BC further downstream, as the isopycnals tend to be higher there due to the densification of the BC, and can therefore reduce in volume.

At the eastern side of the transect in Figures 4.5b-f the isopycnals develop from a horizontal structure (Figure 4.5a), to mostly vertical isopycnals, crossing into the eastern boundary limit. The development of this structure is also observed in Figures 3.4b-h. It is noteworthy, that in Figure 4.5b-c the isopycnals near the eastern boundary limit remain mostly horizontal at the surface, which is unlike the other years, as these have a much more vertical isopycnal structure near the eastern BC. This could be due to the fact that the basin in the first year is not in equilibrium yet, and therefore needs time to adjustment to the (equilibrium) vertical structure.

Finally the velocities in both the eastern and western BC are studied. In the eastern BC the velocity increases from a maximum of 0.4 cm/s in the first year (Figure 4.5a) to a maximum of 0.6 cm/s (Figure 4.5b). In the same year of 3yrDoubleHL, Figure 3.4b, the velocity increases up to a maximum of 0.5 cm/s. Therefore the difference in intensity has a (small) impact on the eastern BC velocity, as the horizontal density gradient is greater in 1yrTripleHL, than 1yrDoubleHL. In the subsequent two years (years 12,13) of 1yrTripleHL, when an average surface heat loss is applied, the velocity reaches its maximum of 0.8 cm/s. This is attributed to the fact that the horizontal isopycnal structure near the eastern BC of year 11, becomes more vertical in years 12 and 13, and thus increases the horizontal density gradient, thus increasing the eastern BC velocity. In summary, the velocity increase in the eastern BC proportionally increases to increased horizontal density gradient near the eastern BC.

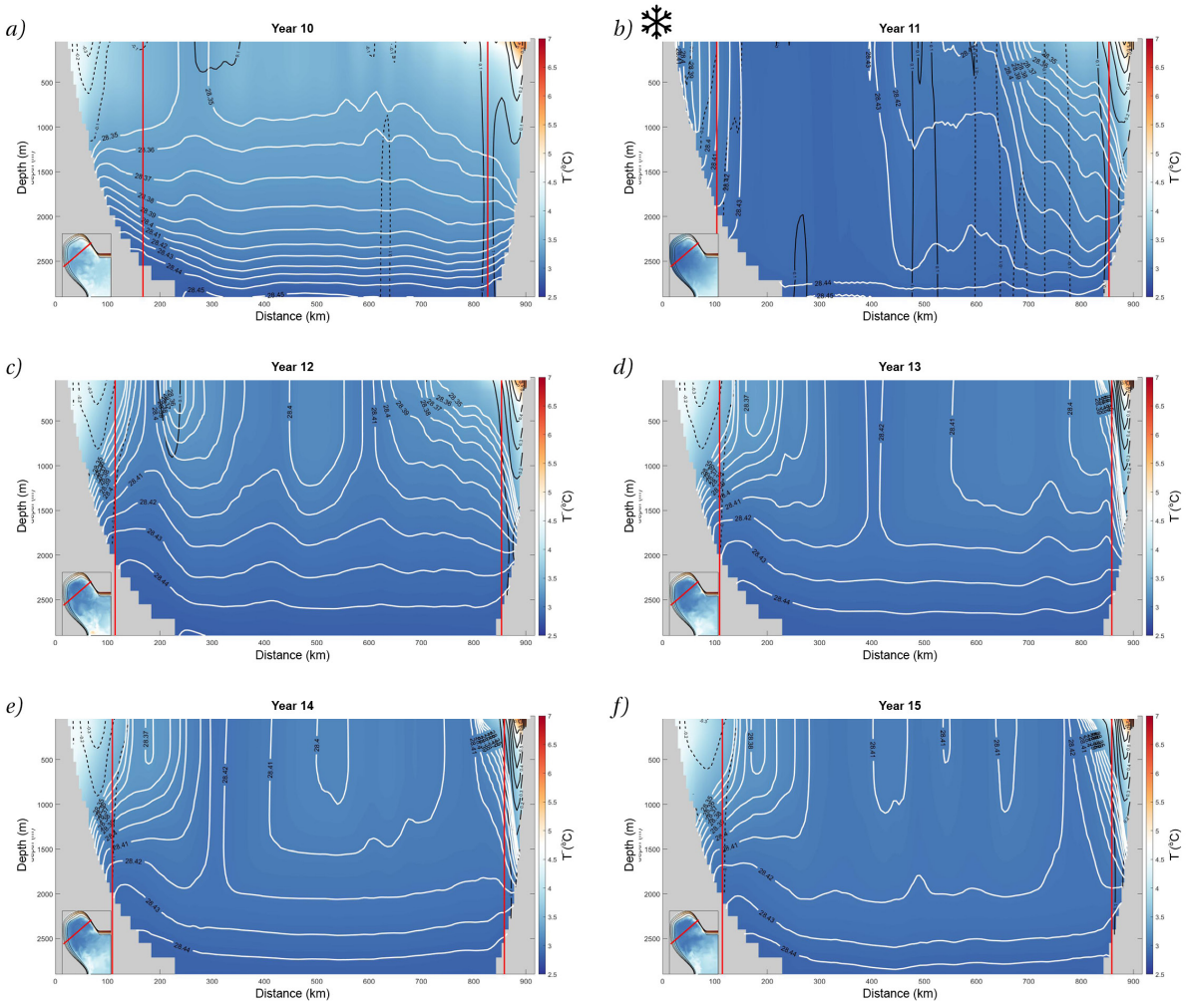

Figure 4.5: a-f) A transect through the convection area, as indicated in the subplot in the bottom left corners, by the red line. The mean temperature of the months February and March of run 1yrTripleHL is plotted for every year and indicated in shading (in °C). The white contour lines define the isopynals, with $\sigma = \sigma - 1000kg/m^3$. The black contour lines indicate the positive velocities and the dashed black lines are the negative velocities, with an interval of 0.1 cm/s. The vertical red lines indicate the limits of the BC based on the barotropic streamfunction, which is fixed at 18 Sv. The year with an extreme winter is depicted by a frost sign.

4.4 Boundary current transport per vertical layer and density class

In previous sections is described how the different interactions change due to an extreme winter. In this section the corresponding change in distribution of BC transport in the vertical and by density class is analyzed to assess changes in the BC structure indicative of overturning and eddy exchange. This is done by looking at the change in transport in two segments of the BC, as defined in Section 2.3.d. A distinction is made between the years with additional surface heat loss (year 11) and the years afterwards (years 12,13 and 14). The segments are the same as in Section 3.4, and are depicted by red lines in Figure 2.4.

First in Table 4.1 is seen how much water is transported through each section per year. It shows that the inflow stays relatively constant in all years. The midpoint has to adjust relatively to the first year and remains constant throughout the years after the additional surface heat loss, this is also the case for the outflow. Noteworthy is that the amount of transport through the outflow increased significantly in the year with additional surface heat loss. A similar results with Table 3.1 is the decrease in the three year average BC transport at the outflow, compared to the central transect transport, and compared to the outflow of the year with additional surface heat loss. Furthermore, the transport through the central transect is smaller than the inflow and outflow transect in Table 4.1. This is attributed to the spin-up time of the basin, as is seen in Section 4.3 the velocity in the eastern BC further increases after the additional surface heat loss year.

Table 4.1: The net transport (in Sv) per year, through the inflow, central and outflow transects from 1yrTripleHL. Highlighted in bold is the year with additional surface heat loss. Note that the transports are negative, as the flow from East to West are in the negative x direction

Year	Sum inflow	Sum middle	Sum outflow
10	-20.32	-14.15	-21.96
11	**-20.59**	**-20.36**	**-24.19**
12	-21.91	-22.12	-20.10
13	-21.41	-22.51	-19.15
14	-20.76	-22.90	-19.16
15	-20.53	-22.30	-19.37
Mean yr 12 - 14	-21.15	-22.46	-19.45

Figure 4.6a shows the difference in transport of water per density class, between the inflow and central transect, of the year with additional surface heat loss (year 11). This figure is almost identical in proportions to Figure 3.6a, with almost the same differences in transport per density class. This suggest that the increased intensity of the winter surface heat loss does not directly influence the overturning in density space in the eastern BC, of the same year. In Section 4.3 something similar is suggested, it suggests that the influence of the increased surface heat loss (compared to a doubling of average heat loss), does not reach the eastern BC in the year of additional surface heat loss. It suggests this is attributed to the fact that the isopycnal structure needs time to adjust to the new basin equilibrium.

Figure 4.6b shows the difference in transport of water per density class, between the central transect and outflow, of the year with additional surface heat loss (year 11). It can be seen how the water of density class $\sigma = 28.33 - 28.5 kg/m^3$ (blue), increases significantly in all layers and a large decrease is seen of density class $\sigma = 27.98 - 28.33 kg/m^3$ (dark orange and yellow). This is likely due to the buoyancy loss to the atmosphere, while traveling through the BC, thus indicating a large overturning in BC, which is also seen in Figure 3.6b, but in smaller proportions. The response confirms what is seen in Figure 4.2, which shows a very high MLD in the BC in this segment. Therefore convection is expected and can be observed as a large overturning in density space in this segment.

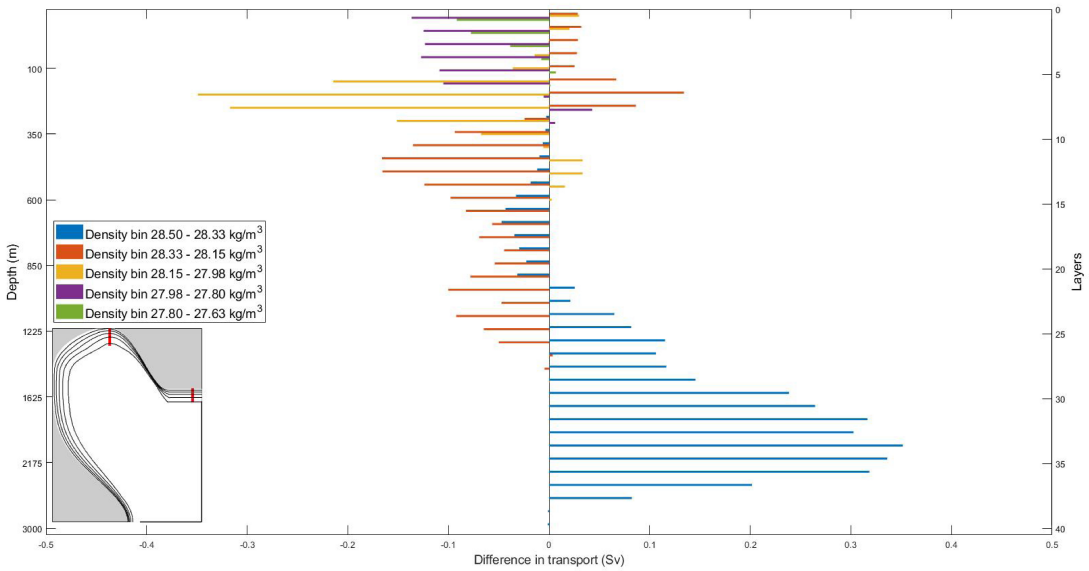

(a)

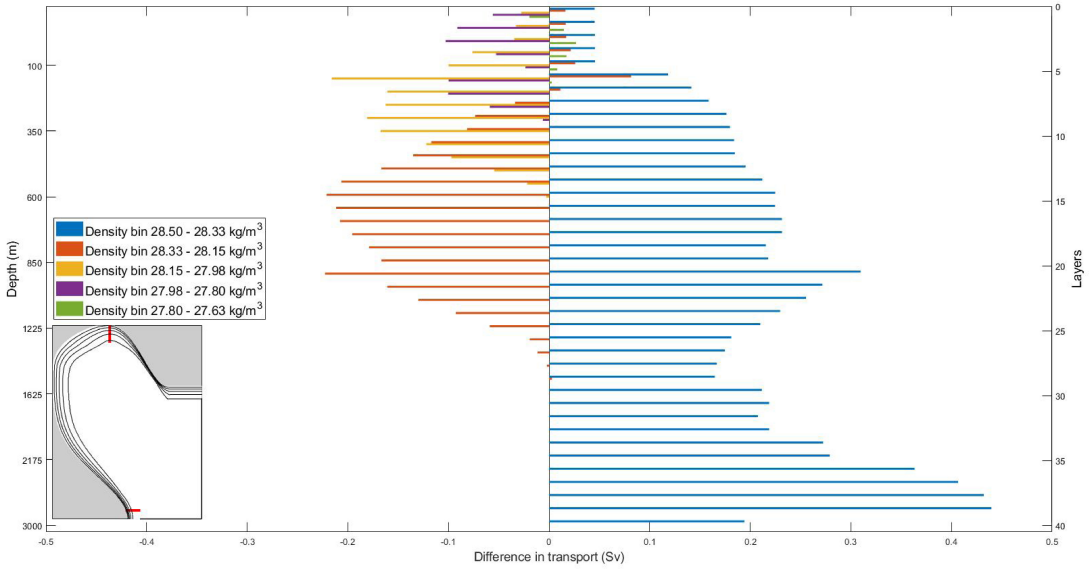

(b)

Figure 4.6: The difference in BC transport per segment of 1yrTripleHL. Plotted as the mean of the year with additional surface heat loss (year 11). The left y-axis is defined as the depth (in m) the right y-axis is defined as the z layers. A positive (negative) difference in transport indicates that the volume of transported water from the density class increases (decreases). a) The segment in the BC between the inflow and central transect. b) The segment in the BC between the central transect and the outflow. Indicated in the subplot in the bottom left corner. The density class of blue is $\sigma = 28.33 - 28.5 kg/m^3$, dark orange is $\sigma = 28.15 - 28.33 kg/m^3$, yellow is $\sigma = 27.98 - 28.15 kg/m^3$, purple is $\sigma = 27.80 - 27.98 kg/m^3$ and green is $\sigma = 27.63 - 27.80 kg/m^3$.

Figure 4.7a shows the difference in transport of water per density class, between the inflow and central transect, averaged over the years with average heat loss (years 12,13 and 14). A very similar pattern as in Figures 3.6a, 3.7a and 4.6a is found. Again, approximately the same amount of dense water from interval $\sigma = 28.33 - 28.5 kg/m^3$ (blue), is added from layer 22 to layer 37 (1000 m to 2475 m depth). Thus, suggesting that the overturning in density space in the eastern BC is constant. In Chapter 5 the BC transport on a seasonal scale is studied to try and better understand what happens in this segment.

Figure 4.7b shows the difference in transport of water per density class, between the central transect and outflow, averaged over the years with average heat loss (years 12,13 and 14). The extreme overturning in density space, as seen by the large increase of the blue density class in Figure 4.6b due to extreme surface heat has stopped in the subsequent years. Similarly as in Figure 3.7b, this segment also has an increase in transport in the upper 12 layers (450 m depth) of the density class $\sigma = 28.15 - 28.5 kg/m^3$ (dark orange). It can be speculated that this transport increase is due to average winter convection, thus overturning the water of the yellow density class into water of the dark orange density class. However it does not explain why there is such a large decrease of the blue density class (also seen in Figure 3.7b), this can be attributed again due to the large difference in total transport through this segment (3 Sv).

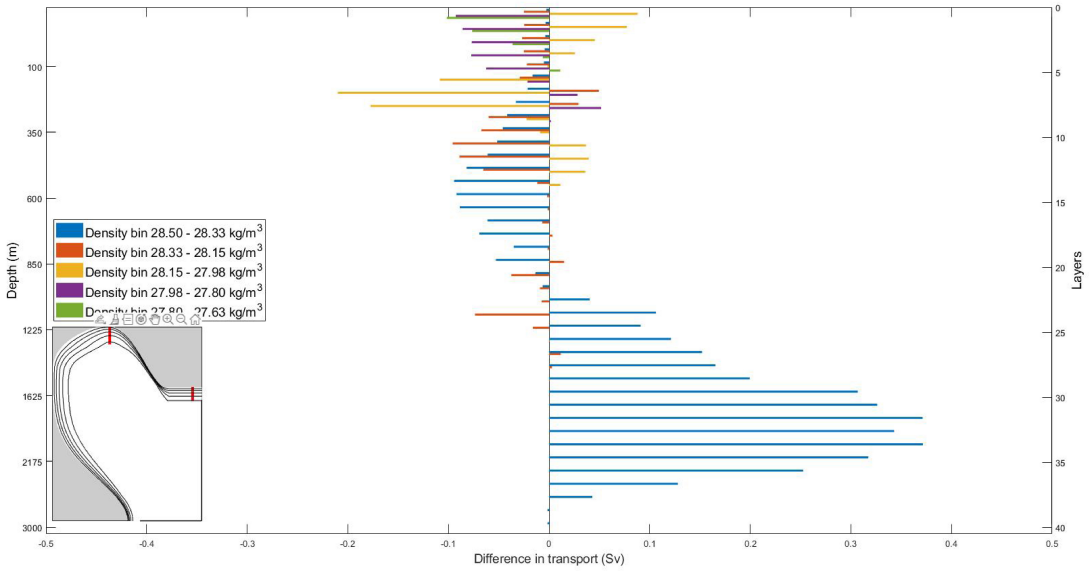

(a)

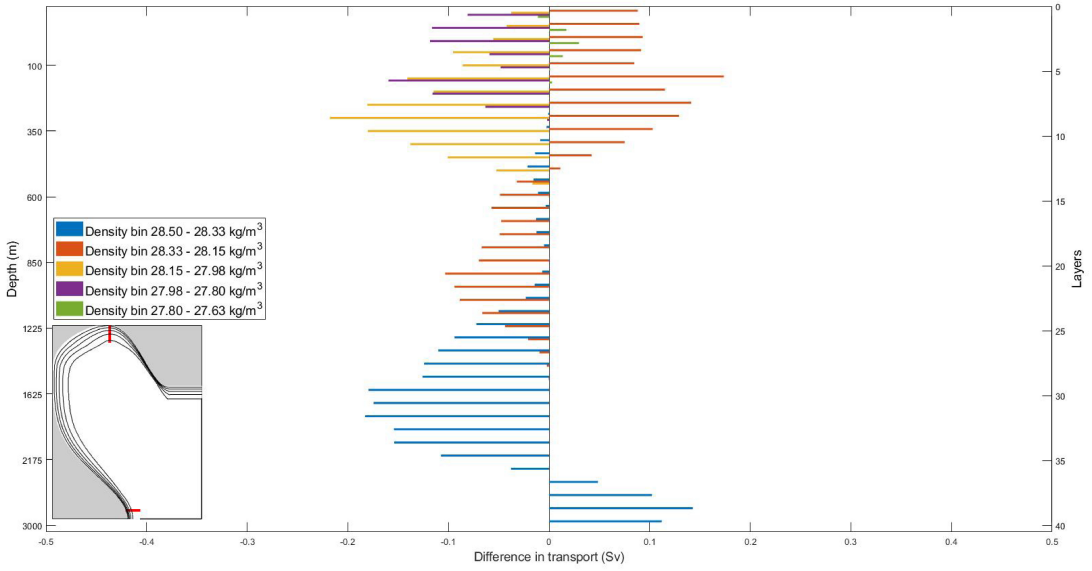

(b)

Figure 4.7: The same as Figure 4.6, but for the years after the additional surface heat loss (years 12,13,14)

5 | Seasonal differences in boundary current transport

This final chapter of results focuses on the effect of additional surface heat loss on seasonal timescales, and specifically on how the transport changes through the eastern BC changes in the short term (per two months). To quantify this change, the focus is on the total BC transport per vertical layer, between the inflow and the central transect. For simplicity, no distinction is made between density classes (it only focuses on the total transport). As explained in Section 2.3.d, the segment is defined at the inflow by a depth limit down to 3000 m, and in the central transect down to 2600 m. Furthermore, seasonality is studied by looking at the months with the weakest and strongest stratification. In the months February and March, the atmospheric cooling of the winter causes the interior to mix and therefore has the weakest stratification. In the summer months, the interior stratifies due to atmospheric warming, and therefore has the strongest stratification at the end of the summer, in the months of August and September. Now that the studied months are established, this is further narrowed down to a number of years to be studied. This is done by looking at the difference in total BC transport per month, plotted for 3yrDoubleHL and REF. From this plot a number of winter and summer months are chosen to be compared to each other. Then two types of comparisons are made, first the winter months are compared to the summer months of both 3yrDoubleHL and REF, with the goal to see what the seasonal differences are per run. Then the winter (summer) months of 3yrDoubleHL are compared to the winter (summer) months of REF, with the goal to study the effect of the additional surface heat loss on both seasons, thus in total four comparisons are made.

In Figure 5.1, the BC transport difference per month between the inflow and central transect is plotted for 3yrDoubleHL (blue) and REF (red). Each data point is defined as all vertical layers summed per month (eg. the sum of the layers from Figures 4.6 and 4.7). Thus, a negative (positive) transport difference indicates that the transport at the inflow is larger (smaller) than the transport at the central transect. The winter months (February and March) are highlighted with red stars. REF shows that in approximately the first six years (month 72 indicated by dashed black line) the transport is low through the central transect in respect to the inflow. After these years the difference varies around 0 Sv. The cause of this large difference is because the viscosity and diffusivity have been changed (Section 2.1) and therefore the basin is not in equilibrium yet. The slow decrease of BC transport difference is attributed to the basin adapting to this new equilibrium. Due to the additional surface heat loss (starting in month 10) of 3yrDoubleHL in years 11, 12 and 13, the transport through the central transect is larger in respect to the transport through the inflow. This difference in transport of 3yrDoubleHL pushes it faster towards the transport difference of 0 Sv. This complements the findings of Chapter 3, which show that both the EKE and the velocity increases in this BC segment as a consequence of the additional surface heat loss. This corresponds to an increase in transport through the central transect, while the inflow remains approximately constant by construction. When comparing the runs to each other, large differences can be found, for example in month 27 the difference in transport is 14.5 Sv, compared to an average transport of 21.5 Sv. Furthermore, maxima and minima of transport differences are expected to coincide based on monthly means, which can sometimes be observed when comparing the winter months, denoted as red stars. But more often than not, maxima and minima do not coincide between the different runs or have a lagged response of one month. Therefore it is concluded that the difference between 3yrDoubleHL and REF in the first six years is too large, but starting in year six the monthly transport difference is relatively small (approximately 2 Sv) and is therefore deemed to be in local equilibrium and is thus suited to be compared to each other.

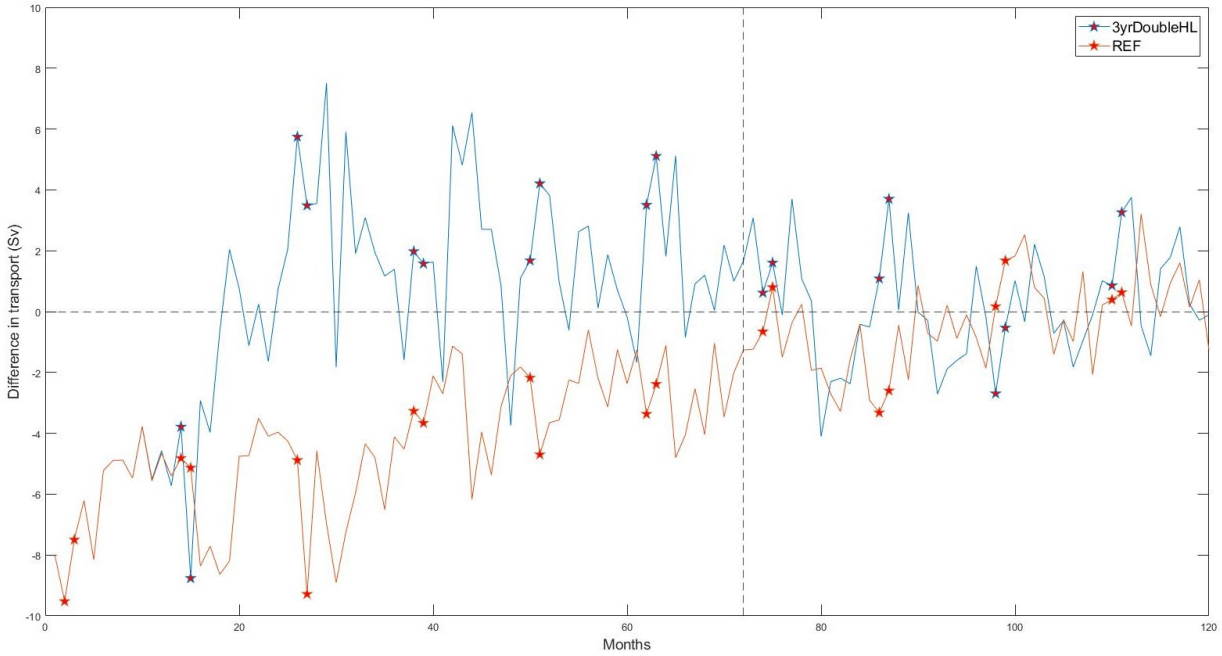

Figure 5.1: The difference in BC transport (Sv) between the inflow and the central transect, for run 3yrDoubleHL (blue) and REF (red) as a function of month number. Winter months are highlighted by red stars (months 14,15,26,27,38,39 are strong winters). The vertical dotted line indicates month 72, starting from this month the BC transport is assumed to be in local equilibrium.

5.1 Comparing BC transport differences at inflow and central transect

First is focused on the differences in BC transport between the summer and winter months of both 3yrDoubleHL and REF. The effects of the strong winter years still persists in the subsequent years and are indicated by an increased EKE (Figure 3.3 and increased horizontal density gradient (Figure 3.4). Therefore, studying the years 16-20 of 3yrDoubleHL is still suited for the goal to better understand what happens between the seasons, and how the lingering effects of the additional surface heat loss affect the seasonality difference. In Figure 5.2a is the BC transport of 3yrDoubleHL averaged over the winter months (dark blue) and summer months (light blue), per vertical layer of years 16-20. The ratio of import to export approximately -1 Sv and thus the total BC transport is smaller at the central transect than at the inflow. During the winter months the export slightly decreases in the upper layers and largely increases in the deeper layers, compared to the summer. Therefore, the ratio of import to export changes to approximately +1 Sv, meaning that during the winter the total BC transport has a larger transport at the central transect than at the inflow.

The same comparison is made for the REF run (Figure 5.2b), for the winter months (dark orange) and summer months (yellow). During the winter of REF, both the export and import increases, compared to the summer. However, contrary to Figure 5.2a, the ratio of import to export stays almost identical for both summer and winter (both approximately -0.5 Sv). Therefore this suggests that the increased EKE and horizontal density gradient in 3yrDoubleHL could have an impact on the proportionality of import versus export during the different seasons.

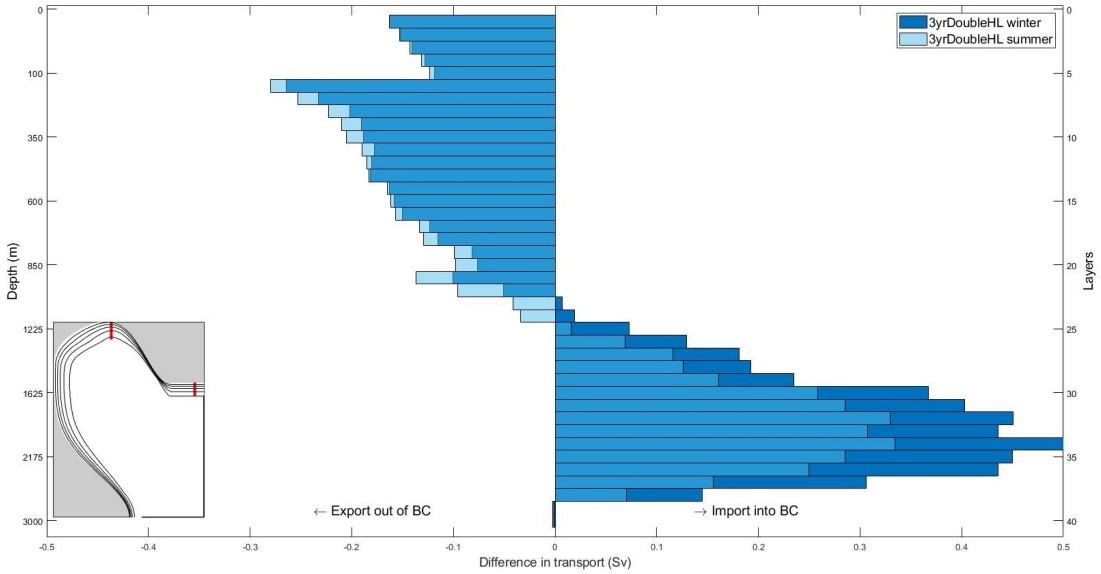

(a)

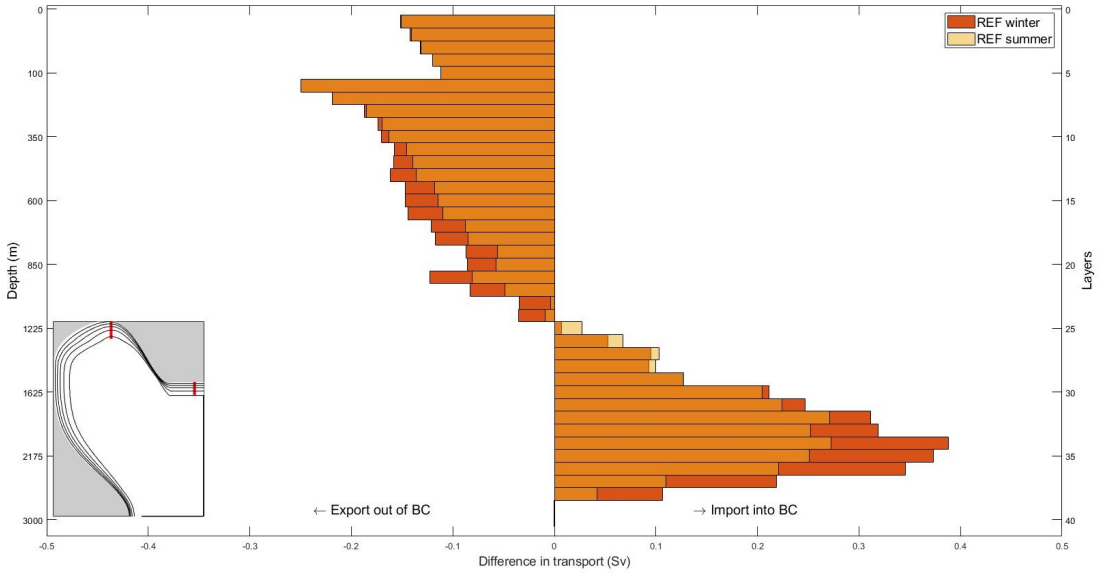

(b)

Figure 5.2: Comparison of the difference in BC transport per vertical layer (Sv) and depth (m), between the inflow and central transect of years 16-20. a) Average of 3yrDoubleHL, of the winter months (February and March in dark blue), and summer months (August and September in light blue). b) Average of REF, of the winter months (dark orange) and summer months (yellow).

Now the same distributions of Figure 5.2 are plotted, but the winter (summer) months of 3yrDoubleHL are compared to the winter (summer) months of REF. In Figure 5.3a is the BC transport plotted, of the winter months of 3yrDoubleHL (dark blue) and of REF (dark orange), per vertical layer of years 16-20. The export of surface BC water is slightly larger in the winter of 3yrDoubleHL run than the winter of REF, while the import in the deeper BC layers is much larger in 3yrDoubleHL.

The same comparison is made for the summer months (Figure 5.3b), for 3yrDoubleHL (light blue orange) and REF (yellow). The increase in export in the upper layers is larger than the increase in import in the deeper layers of 3yrDoubleHL, compared to the summer of REF. This difference however is not large. In the next paragraph these results are studied in more detail and related to a transect of the eastern BC.

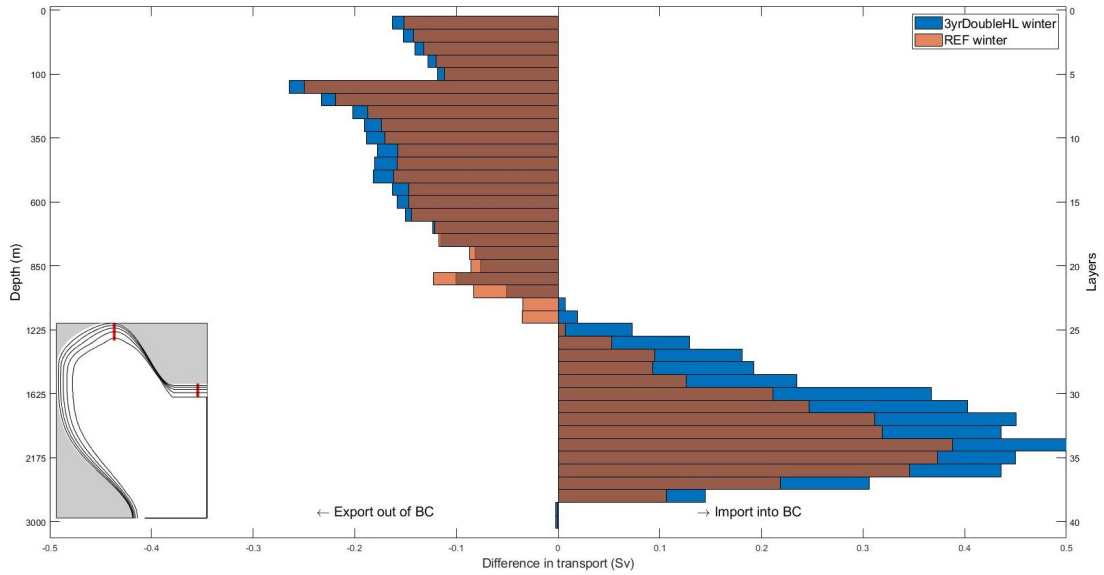

(a)

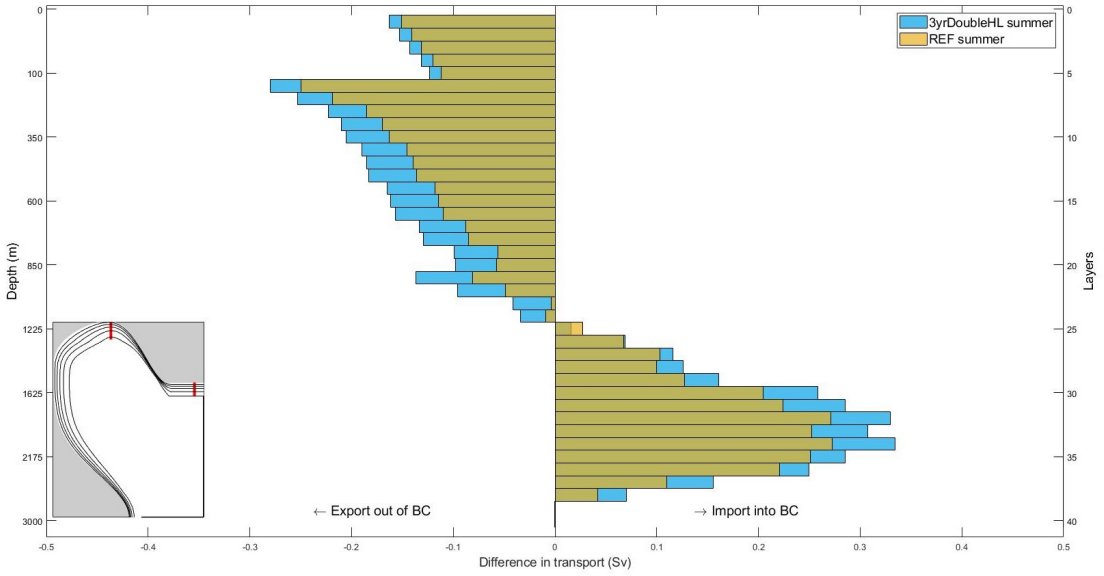

(b)

Figure 5.3: Comparison of the difference in BC transport per vertical layer (Sv) and depth (m), between the inflow and central transect between 3yrDoubleHL and REF of years 16-20. a) Averaged over the winter months (February and March), 3yrDoubleHL (blue), REF (dark orange). b) Averaged over the summer months (August and September), 3yrDoubleHL (light blue), REF (yellow).

From these comparisons it can be concluded that when the basin is cool the overall exchange intensifies, either both the import and export increases, or only the import in the deep layers increases. To gain more insight why this difference is observed, two transects are taken of the eastern BC in these seasons. In Figure 5.4a the wintertime transect and in Figure 5.4b the summertime transect is shown from 3yrDoubleHL in year 16 as an example. The white isopycnal lines show the first important difference. In both seasons the isopycnals range from $\sigma = 28.14 kg/m^3$ to $\sigma = 28.42 kg/m^3$, with intervals of $\sigma = 0.04 kg/m^3$. As can be seen in Figure 5.4b, the stratification in the interior is much stronger in the summer than in the winter (Figure 5.4a). However, within the eastern BC, the isopycnals are almost identical when comparing the seasons to each other. Additionally, it can be observed that the eastern BC velocity is higher in the wintertime than in the summertime (velocity contours, depicted as black lines). In Figure 5.4a the velocity contour line of $u = 0.1 cm/s$ of the wintertime extends to the bottom of the BC and it reaches a maximum of $u = 0.8 cm/s$, whereas in the summer the contour line of $u = 0.1 cm/s$ does not reach the bottom and a maximum of $u = 0.7 cm/s$ is reached. An increase in velocity due to cooling is previously observed in Chapters 3 and 4, and it was suggested that due to the increased BC velocity, more eddies are shed from the BC. Therefore it is deemed most likely that the increase in exchange in the eastern BC as seen in Figures 5.2 and 5.3, is related to the increase in number of eddies shedding into the interior. These eddies could be the cause of the increase in import at depths of approximately 1225 m and deeper (Figures 5.2 and 5.3), when comparing this to Figure 5.4, it suggests that the water with a density of $28.3 kg/m^3$ and denser is able to flow along the isopycnals from the interior into the BC in both seasons. However, to relate the increase of eddies to the increased exchange is difficult on the studied timescales. The eddies are shed on a timescale of days, whereas the transport and transect is studied as an average of multiple months. Additionally, Figure 5.1 shows how variable the BC transport can be on a monthly scale. Therefore no clear explanation can be given on how the eddies exactly affect the exchange. Theories about the diversion of eddies along regions of increased MLD (Section 3.2) could be related, as the eddies might not be able to export more water out of the surface, but are able to import more water from the deeper layers (seen in Figure 5.2a and Figure 5.3a). However, with the current data this can not be studied sufficiently and could be a focus point for a next study by for example applying Lagrangian particle tracking on the eddies, to better understand how water particles behave. Or alternatively study a shorter timescale than months to get more insight on how the eddies interact with the basin.

In summary, it has been concluded in this chapter that an increase in import is observed during wintertime, compared to summertime, in 3yrDoubleHL and REF (Figure 5.2). This is also confirmed when comparing the wintertime of 3yrDoubleHL to REF (Figure 5.3a). However when comparing the summertime of 3yrDoubleHL and REF (Figure 5.3b), it shows an increase in import and export relative to REF. These comparisons have one thing in common; when the basin is cool the overall exchange intensifies, either both the import and export increases, or only the import in the deep layers increases. In Section 3.2 it is concluded that due to a colder interior (increased horizontal density gradient), the velocity in the BC increases, and therefore more eddies are shed into the interior and therefore increase the eddy exchange. It is speculated the increase in eddies is likely the cause of the increased exchange. However the exact relation between the increased exchange and increased number of eddies is not found, and could be a the focus point for future research.

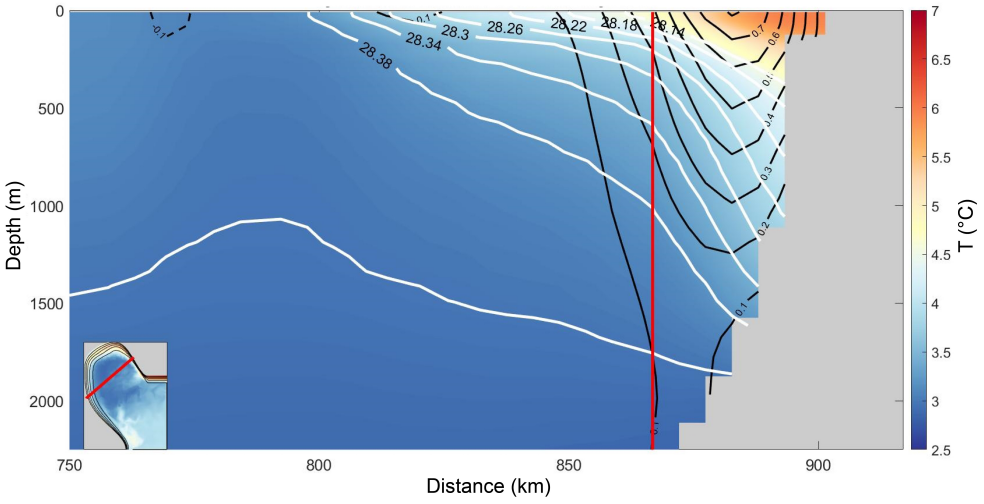

(a)

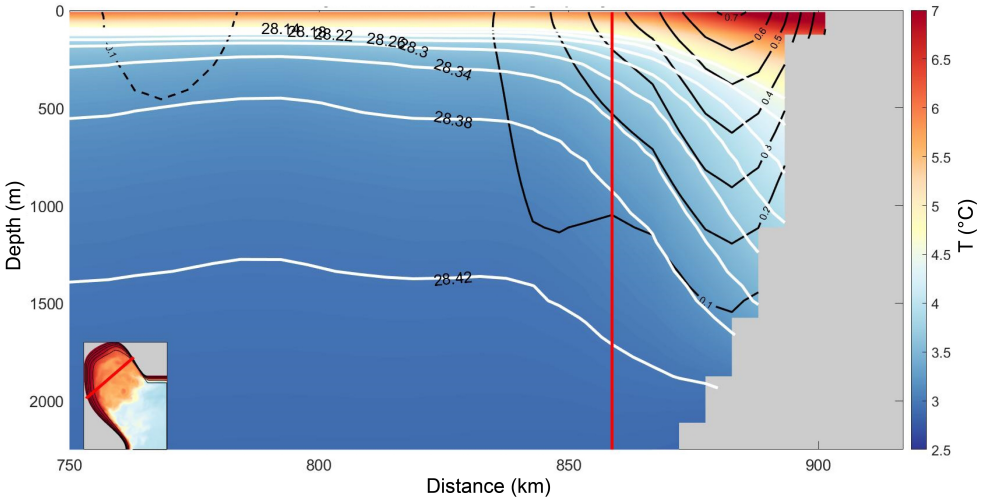

(b)

Figure 5.4: A comparison of the eastern BC of3yrDoubleHL in year 16, a) mean wintertime transect (February and March) b) mean summertime transect (August and September). The mean temperature is indicated in shading (in °C). White isopycnal contour lines ranging from $\sigma = 28.14 - 28.42 kg/m^3$, with intervals of $\sigma = 0.04 kg/m^3$. Black contour lines indicate the velocities, with intervals of $0.1 cm/s$. The vertical red lines indicate the limit of the BC based on the barotropic streamfunction, which is fixed at 18 Sv.

6 | Discussion and conclusion

In this chapter the research question and sub-questions will be addressed and discussed, by interpreting the results from Chapters 3, 4 and 5. The first section is on how the dynamics of the Labrador Sea adjust to wintertime heat loss, in respect to timescale (Sectino 6.1). The second section is on the dynamics of the Labrador Sea in relation to the duration and intensity of wintertime heat loss (Section 6.2). Next, the seasonal differences in the eastern BC are addressed (Section 6.3). Then the results of this thesis are compared to the OSNAP measurement studies (Section 6.4. Finally, the main findings in context of the main research question are summarised in a flow chart. In every section the results will be put in context to established theories and earlier research, then a conclusion will be drawn and a discussion is formulated.

The main aim of this research was to see how the dynamics of the Labrador Sea are affected by extreme (consecutive) wintertime heat loss. With the goal to better understand the processes in the Labrador Sea, and therefore better understand the AMOC. The data to research this is gathered by using an idealised configuration of the Labrador Sea, where the hydrostatic primitive equations of motion are solved on the MIT general circulation model (MITgcm). Different type of scenarios are made to analyse different effects on the dynamics. These scenarios are analysed by looking into how the mean basin temperature changes, how the eddy kinetic energy (EKE) and mixed layer depth (MLD) develop, and how the properties through a transect of the basin change. The effects of these interactions are then studied by looking at how the transport of water per density class and per vertical layer change throughout the boundary current. With these results the main research question can be answered:

How does winter surface heat loss influence the composition and export time scale of the Labrador Sea Water?

6.1 How do the processes governing the Labrador Sea Water (boundary current-convection- and eddy field), adjust to the wintertime heat loss?

The goal of this sub-question is to better understand on what timescales the dynamics of the Labrador Sea react to the additional surface heat loss during wintertime. Johnson et al. (2019) summarises, what the key processes of the formation of Labrador Sea Water are (Figure 1.2). Depicted as (b) in this figure is the buoyancy loss due to heat loss. In the simulations this heat loss is amplified during the months November to March, which causes both the BC and interior to lose buoyancy (Figure 2.1). The effect of the buoyancy loss, depicted as (c) in Figure 1.2, is the cause of deep convection in the interior. The process of deep convection, illustrated in Figure 1.1b, is a process that spans over multiple months (Marshall & Schott, 1999). Deep convection causes the interior water to mix and reaches its maximum mixed layer depth at the end of the winter months in February and March, when the interior has been affected the longest time. Figure 3.3 shows that when additional surface heat loss is applied the MLD increases compared to an average winter (REF). This is most evident in the interior and in the western BC. Comparing the MLD in the interior of 3yrDoubleHL to REF in February and March (Figure 3.3b-d), shows that the MLD locally is 2000 m deeper in the interior, and in the western BC 500 m deeper than REF. Similar results are found by Georgiou et al. (2020), which show a direct correlation between the response of the MLD and a change in heat flux. The consequence of an increased MLD during the winter is that more water is being convected. This is illustrated in Figure 3.4b-d, which shows a vertical isopycnals structure, with densities up to $\sigma = 28.45 kg/m^3$ in the interior. This is equivalent to an increase of convected water in the deeper layers that is relatively cold (and dense), and thus reducing the yearly mean temperature of the basin, as shown in the mean basin temperature (Figure 3.1). This is affecting the next winters, as this volume of deep cold water largely remains in the interior. If the next winter is strong, the MLD reaches the transformed dense water of the previous strong winter and cools it down further. If the next winter is average the MLD does not reach the highest density classes, but reaches depths dependent on how many consecutive strong winters occurred. If the convected water is transported back into the BC through lateral spreading, it will flow out of the basin on a timescale of months to a maximum of two years (Georgiou et al., 2020).

Due to consecutive strong winters dense water accumulates in the deeper parts of the basin. The resulting accumulation is observed in the last four years of the transect of 3yrDoubleHL in Figure 3.4e-h. The volume of water in the bottom layer slowly reduces throughout the years. In Figure 3.4e-h the water with a density of $\sigma = 28.44 kg/m^3$ is not able to cross into the BC, but the water slightly more buoyant is able to cross into the deep layers of the BC. This indicates that all water lighter water than $\sigma = 28.44 kg/m^3$ is able to exchange with the BC, but that the reduction of the densest water at the bottom can not be attributed to a BC exchange at this specific location. However, a year to year reduction is still observed. Diapycnal mixing is weak in this area, as there is the external source of energy that induces the mixing at these depths is small. It could be possible that during summer (or other) months the densest isopycnal is able to cross into the BC, which causes the small yearly decrease. However, transects from specifically the summer months have confirmed that mostly the upper half of the basin is affected due to the summertime heat flux (Figure 5.4), and therefore does not affect the water with densities of $\sigma = 28.43 - 28.44 kg/m^3$. So what is deemed most likely, is that the majority of the water is transported out of the interior due to a pressure difference. The water at the western side of the interior is affected the most by a strong surface heat loss, thus in this area the largest volume of dense water is accumulated. In the eastern part of the interior the effect of the surface heat loss is significantly smaller, and therefore has a smaller volume of relatively more buoyant water at the bottom. Thus a baroclinic flow from the west to the east is formed, slowly removing the densest water volumes of the interior. Alternatively, as the densest isopycnal almost crosses into the western BC (Figure 3.4e-h) it can be speculated that during other months, or in other areas of the basin, this water is able to leave through the BC.

Next the eddy exchange is studied by looking at the eddy kinetic energy (EKE). The EKE is based on the turbulent velocity components, which is influenced by the instantaneous and average velocity. The eddy exchange is depicted as (d) in Figure 1.2. The EKE increases significantly compared to the REF run in the eastern part of the BC (Figure 3.3b-d). The EKE pattern suggests that the eddies can not shed into the interior easily, as a strong front is formed at the eastern BC limit, as seen in the transect of 3yrDoubleHL in Figure 3.4b-d. During a strong winter the horizontal density gradient between the BC and interior is higher, compared to an average winter, based on the thermal wind balance this means that the velocity in the BC in downstream direction increases. In the summer when the interior is stratified again, the horizontal density gradient is much smaller. Therefore, during the winter the velocity in the BC is larger than in the summer, which is shown in Figure 5.4. Due to the velocity increase the BC becomes more unstable and the number of eddies increase. However, due to the strong front near the BC during the winter, these eddies have difficulty going offshore and are therefore focused in the BC (Figure 3.3b-d). In conclusion, the larger the MLD is, the more difficult for the eddies to shed into the interior and are therefore focused inside the BC. Subsequently, as the MLD only decreases partially after the extra strong winters, the EKE therefore stays relatively enhanced (Figure 3.2d-h). Therefore, the increased EKE in the BC is not only in the year of additional surface heat loss, but also in the years afterwards.

The adjustment of MLD and EKE have an effect on the BC transport. The transport of water per density class in the strong winter years (Figure 3.6a) confirms the exchange between the eastern BC and interior, as is also concluded from a modeling study by Brüggemann & Katsman (2019). It is seen that annually a large increase of dense water (blue in Figure 3.6a) from interval $\sigma = 28.33 - 28.5 kg/m^3$ is found in the bottom layers, between the inflow and central transect, and a large decrease of water from interval $\sigma = 27.63 - 28.33 kg/m^3$. The previous paragraph concludes that during the winter (in February and March) the exchange between the interior and BC is prevented by the strong front. Therefore the exchange that is observed in Figure 3.6a has to happen during another time period. It is expected that the exchange happens after the summer months, when the interior has restratified. This causes the isopycnals near the BC to be less steep and could allow for the exchange. However, Chapter 5 does not show an increase in exchange in summertime. In Section 6.3 this seasonality difference is further discussed in detail.

It should be noted that in the years with average winters, as seen in Figure 3.7a, the overturning in density space proportions are almost equal to the years with strong winter, as seen in Figure 3.6a. It indicates that the increase of surface heat loss in the winter, has long term effects in the eastern BC segment. This is attributed to a prevailing high MLD in the subsequent years after the strong winters and causes the EKE to remain high.

Finally, the transport of water per density class in the segment between the central transect and outflow indicates overturning in density space. As seen in Figure 3.6b in the years with strong winters, a large volume of water of interval $\sigma = 27.98-28.33 kg/m^3$ is removed, and an almost equally large amount of the of water in density class $\sigma = 28.15-28.5 kg/m^3$ is added. This indicates that the respective waters are locally convected due to surface heat loss, as the surface heat loss is locally largest in this segment. In the years with average winters (Figure 3.7b) the large influx of the densest water with density $\sigma = 28.33-28.5 kg/m^3$ is not observed. However, a large increase of water with density $\sigma = 28.15 - 28.33 kg/m^3$ is added in the upper layers. This water could be the result of water with density $\sigma = 27.98 - 28.15 kg/m^3$ being locally convected, but has not had sufficient time to flow to deeper layers. But, in Table 3.1 is seen that the net transport from the central transect to the outflow has a difference of 3 Sv, which is a significant difference. This could be the reason for the large decrease in densest water in the lower layers, which is unexpected. To better investigate what happens in this segment the defined segment could be defined differently, eg. not depth limited but transport limited. Or alternatively a Lagrangian particle tracking could be used to study what exactly happens with the dense water particles in this segment, as it has been proved to be a powerful tool to study the pathways of convected water particles (Georgiou et al., 2020).

6.2 Considering the adjustment times of the dynamics, do the changes in dynamics scale with the duration and intensity of extreme wintertime heat loss?

The focus in this paragraph is on how the number of consecutive winters affect the processes governing the LSW. The number of consecutive strong winters has a direct influence on the MLD in the subsequent years for the entire simulation period. This is observed in Figure 3.4b-d, where the vertical isopycnal structure reaches the bottom during the third strong winter. In the subsequent years (Figure 3.4e-h) the vertical isopycnal structure in the upper layers in the interior remain on average up to depths of 1500 m. The vertical isopycnal structure at the upper layers in the interior after one strong winter (run 1yrDoubleHL), remain on average up to depths of 2000 m. The vertical isopycnal structure in the interior after five strong winters (run 5yrDoubleHL), remain on average up to depths of 1000 m. In summary, the convected dense water after a single strong winter has not left the basin yet. Therefore, as the number of consecutive strong winters increases, the volume and density of the convected water of the previous year increases, as it is cooled down further every strong winter. To gain more insight on how this convected water exactly behaves, a Lagrangian particle study can be conducted to see if it leaves the basin near the bottom, due to a pressure difference. Or it is possible that the convected water is able to cross further downstream back into the BC, as the isopycnals tend to be higher there. Therefore different transects through the basin could be investigated, to determine if the crossing of densest water into the BC is possible in other locations.

To address the effect of the intensity the focus is now on the difference between 1yrTripleHL, 1yrDoubleHL and REF run. It is observed in Figure 4.4b that the difference in MLD between 1yrDoubleHL and 1yrTripleHL is most evident in the western BC, where it exceeds 1000 m. The difference is attributed to the increase in heat loss over the western BC. This results in a large overturning in density space, as a large increase of the densest water over the entire depth can be observed in the western BC (Figure 4.6b). Furthermore, the increased intensity of 1yrTripleHL shows that the water that is convected is denser than the convected water in the same year of 1yrDoubleHL. This is observed by comparing Figure 4.5b to 3.4b, which show that the interior water has indeed a higher density. Thus, the interior is colder and denser and therefore the horizontal density gradient is larger, thus an increased BC velocity should be observed. However the increase in BC is not observed in Figure 4.5b, this is attributed to the fact that the convection is focused near the western BC, where the heat loss is highest. Therefore no immediate response in the eastern BC is observed, as the convection area is too far away from the eastern BC to affect the velocity. This could be due to spin-up time of the model as subsequent years (Figure 4.5c-f and 3.4d-h) tend to have a steep isopycnal structure near the eastern BC. It suggests that the isopycnal structure seen in Figure 4.5b and 3.4b is still adjusting to the equilibrium. Or it could be, that the convective plume near the western BC needs time to laterally spread and therefore on a longer timescale affect the isopycnals near the eastern BC. This can be resolved in future research by starting the simulation in the basin equilibrium state.

The impact of the intensity difference is shown to have a negligible effect on the EKE and MLD on the long term (Figure 4.4c-f). These figures show that the difference between MLD and EKE in the winter months of 1yrDoubleHL and 1yrTripleHL are small and thus suggests that both runs recover with the same magnitude and speed. Although the interior is colder in all remaining years of 1yrTripleHL, it does not have a lasting effect on the MLD, and therefore the EKE. This is likely due to the fact that the intensity increase of 1yrTripleHL, compared to 1yrDoubleHL, is focused in the western BC (Figure 4.4b). The majority of the convected BC water is likely directly exported out of the Labrador Sea through the BC, and therefore does not affect the basin on a long timescale. In conclusion this suggests that there is a limit to the long term effects of an increased intensity of surface heat loss. There is likely a point inbetween a doubling and tripling of the average heat loss, where the additional convected water is not able to laterally spread throughout the basin, but is removed out of the basin through the BC, within the same year. This could be confirmed in future research by applying Lagrangian particle tracking in the convection area and apply the tripling of average winter surface heat loss.

Preferably a longer period of tripling heat is applied, but unfortunately this was not feasible, as the model became unstable after two consecutive extreme winters. However, a run that applies an average year of heat loss inbetween two extreme winter years remained stable, resulting in the AltTripleHL run (and additionally, with a less extreme winter, the AltDoubleHL run). Although not shown in this thesis, the interactions between different dynamics do not fundamentally differ. An increased MLD and EKE is seen in the years of additional surface heat loss, which confirms previous results of the time and intensity based runs.

6.3 Seasonal differences in boundary current transport

In Chapter 5 is observed that during the winter a larger exchange than in the summer occurs in the eastern BC segment. This segment is characterised by a strong eddy field. The decrease in export in the surface layers, and the increase in import in the deeper layers is mostly attributed to the eddy exchange as theorised in Brüggemann & Katsman (2019). Convection due to heat loss, and therefore diapycnal mixing in this part of the BC is present at shallow depths and is negligibly small. Therefore, the conclusions are mostly related to how the eddy behavior changes. In total four comparisons are made to study the seasonality differences. Additionally, from Figure 5.1 is concluded that the seasonality studies will be focused on the last four years of the simulation period. In these years the BC transport in 3yrDoubleHL and REF are in equilibrium and can therefore be compared. In the first six years the BC is not in equilibrium yet, and therefore the runs have different characteristics.

In these runs the average difference in BC transport per vertical layer are compared, for the two extreme cases of stratification. In the winter the interior has the largest MLD and is dependent on how many consecutive strong winters occurred. The mixed water is a lot denser than the BC water, and therefore a strong front, just outside the BC is present. The front of 3yrDoubleHL is stronger than the one of REF, as the additional surface heat loss in the earlier years still has an effect on the basin in the subsequent years. The isopycnal structure between 3yrDoubleHL and REF inside the BC does not significantly change. During the summer the interior stratifies again, therefore removing the strong winter front near the BC. In 3yrDoubleHL the mean basin temperature is colder than REF, thus has denser isopycnals near the surface. However the isopycnal structure in the interior and BC is very similar. Additionally it should be noted that inside the BC, the isopycnal structure barely changes between summer and winter, as seen in Figure 5.4. These findings are summarised in Table 6.3 and are compared in the following paragraph.

Table 6.1: Summary of main differences of 3yrDoubleHL and REF per season. In the outer rows and columns the seasons and runs are compared to each other.

	Winter	**Summer**	**Winter vs. summer**
3yrDoubleHL	Strong front	Stratified, with dense water at the bottom of the interior	Enhanced import in winter
REF	Moderately strong front	'Normally' stratified	Enhanced import & export in winter
3yrDoubleHL vs. REF	Enhanced import in 3yrDoubleHL	Enhanced import & export in 3yrDoubleHL	

First, the winter and summer months are compared, of the runs 3yrDoubleHL (Figure 5.2a) and REF (Figure 5.2b). The comparison shows the water in the deeper layers increases the most in the winter, compared to the summer. A variability in the upper layers is observed, where in 3yrDoubleHL the amount of water decreases in the upper layers, and in REF increases (but is focused in the middle layers). A similar trend is observed in Figure 5.3a, which compares the 3yrDoubleHL winter and REF winter to each other. Again a large increase in import is observed in the deeper layers, while a small increase and decrease in export is found in the upper layers. However, it is not necessary that the import and export have to be equal, as can be seen in Figure 5.1 the difference in transport in the eastern BC is highly variable and is almost never exactly zero. It is concluded that when the basin is cool the overall exchange intensifies, either both the import and export increases, or only the import in the deep layers increases. Additionally, an increased velocity in the BC in the downstream direction in wintertime is found, which indicates an increase in eddies. It is therefore likely that the increase in number of eddies is the cause of the increased exchange. Furthermore, in Section 3.2 is theorised that the eddies shedding from the eastern BC deviate along the area of increased MLD during wintertime, as a strong front is present. This might suggest that due to the change in direction (more downstream directed), the eddies are not able to export more water out of the surface, but are able to import more water from the deeper layers (seen in Figure 5.2a and Figure 5.3a). However, with the current data this can not be studied sufficiently and could be a focus point for a next study. Therefor, in future studies I suggest to apply only an average surface heat loss and then look into the seasonal differences, as the BC should be in stable equilibrium then for a longer time, and therefore a less variable transport study can be done. Another type of study that could further help analysing the seasonal differences, is a Lagrangian particle tracking study in this region. I therefore suggest to release the passive tracers at the outflow of the BC or in the convection area and study the particles that cross into the interior and back into the BC in the eddy region, then by isolating the water particles per season, it could provide insight into how the eddy exchange exactly behaves per season.

6.4 Can the results of the idealised model help to interpret variability in Labrador Sea Water export, as seen in observations?

As stated in Chapter 1 the inflow and outflow of the Labrador Sea are measured at the locations as seen in Figure 1.3 and are presented and discussed in Holliday et al. (2018). The focus in this article is on estimating the circulation, volume and property transport through the Labrador Sea. In other words it measures what comes in and out of the Labrador Sea, and it does not provide data on how the dynamics inside the Labrador Sea transform the LSW. This thesis tries to provide the data on how the dynamics affect the LSW formation and specifically tries to better understand what happens in the Labrador Sea and provide insight on what time- and spatial scales the dynamics behave. This thesis outlines how the basin changes due to additional surface heat loss and gives insight in the complexity of the system as each dynamic interacts with each other on variable timescales. Additionally, Figure 5.1 shows how variable the eastern BC transport can be, which reaffirms the complexity of the system and its non-linearity. Finally, although the idealised configuration captures the physical processes that are essential to producing LSW, it still has its limitations, as is best described in Georgiou et al. (2020). Therefore, it implies that a direct comparison of the presented data and the measured data of Holliday et al. (2018) is not well suited, as the methods and variables used to study the formation of LSW in this thesis are almost not comparable. Although no quantitative comparison can be made, a number of recommendations can still be formulated in a qualitative manner, to provide a more practical application of this thesis.

Firstly, the response time of the net transport through the BC after the additional surface heat loss year(s) has an immediate effect. It can be observed in Tables 3.1 and 4.1, that the outflow increases in the years with additional surface heat loss, compared to the years after the additional surface heat loss, where a decrease of transport is observed in the outflow. Although these averages have a relatively large yearly variability, it shows that the response of a strong winter is a larger transport at the outflow in the same year(s), and a smaller transport in the year(s) afterwards at the outflow. However, as seen in Figure 5.1, a large variability in monthly transport in the eastern BC segment is observed, which is also observed in Tables 3.1 and 4.1. Therefore, it suggests that the effects of a strong winter should be noticeable in the long term when measuring total transport through the outflow, when averaged over a long time series. This increase in transport through the BC would be attributed to the increase in horizontal density gradient, causing an increase in velocity in the BC. To test if this hypothesis is correct a different transect should be measured than the current OSNAP transect from WGC to LC. It would be recommended to measure a similar transect as in Figure 2.4, which contains the eddy field, the area with the highest heat loss and the interior where the MLD is largest. With this transect the hypothesis on the accumulation of dense

interior water and the EKE and MLD interaction can be tested. It should be highlighted that preferably these measurements should be done at a prolonged timescale, as the monthly variability is large and can therefore be reduced.

In previous work of Brüggemann & Katsman (2019) and Georgiou et al. (2020), the importance of the eddy exchange on the overturning of AMOC water is highlighted. New insights from Chapter 5 show that the eddy exchange is highly variable and has a large seasonal dependence. Therefore a similar measurement through the central BC transect (Figure 2.4), can provide further insight into the development of the density structure, to specifically measure what the influence of the eddies are on the overturning in the BC.

To summarise the outcome of this thesis, a flow chart is presented on how the different processes in the Labrador Sea respond to an increase in wintertime surface heat loss (Figure 6.1). The following paragraph explains the elements of the flow chart. Starting on the left side with the black square, representing the additional surface heat loss in a strong winter. As a result of the increased heat loss, convection inside the western BC occurs during the winter months, which can be seen by following the lower path of the chart (second row of the blue column). The consequence of the convection is overturning in density space in the western BC, this water is then directly exported through the western BC and causes an increase in transport (compared to an average winter) throughout the rest of the year, (third row of the purple column). Another consequence of the increased heat loss, is the immediate impact on the MLD in the interior (first row of the blue column), as the water convects into the deeper part of the basin. The increased MLD causes the eddies to be redirected along the area of increased MLD, due to the strong front that is formed within the interior, near the eastern BC. It is shown that the increased EKE in the BC is not only present in the strong winter years, but remains over the simulation period (second row of the purple and orange column), due to the interior staying relatively cold in the subsequent years, causing a large horizontal density gradient. Subsequently an increased MLD means that more dense water accumulates in the interior (first row of the purple column). The combination of the accumulated dense water in the interior and the increased EKE through the BC has two effects. The first effect is that the EKE can not exchange the densest convected water near the bottom of the basin with the BC. Thus the accumulated densest water stays dormant near the bottom of the basin until the next strong winter, when the MLD reaches it again, and cooling it further. Therefore reinforcing the process (purple arrow). The second effect is related to the constant large MLD and high EKE throughout the simulation period, as the horizontal density gradient remains large, it causes the velocity of the eastern BC to also remain relatively high, which in affects the long term export of water through the BC (first row of the purple and orange column). Finally, due to the fact that the densest water is not able to be exchanged with the BC, it slowly flows near the bottom out of the basin due to a pressure difference. Therefore this is a multi-year response, which acts as a negative feedback to the consecutive winter, as it decreases the volume of densest water (orange arrow).

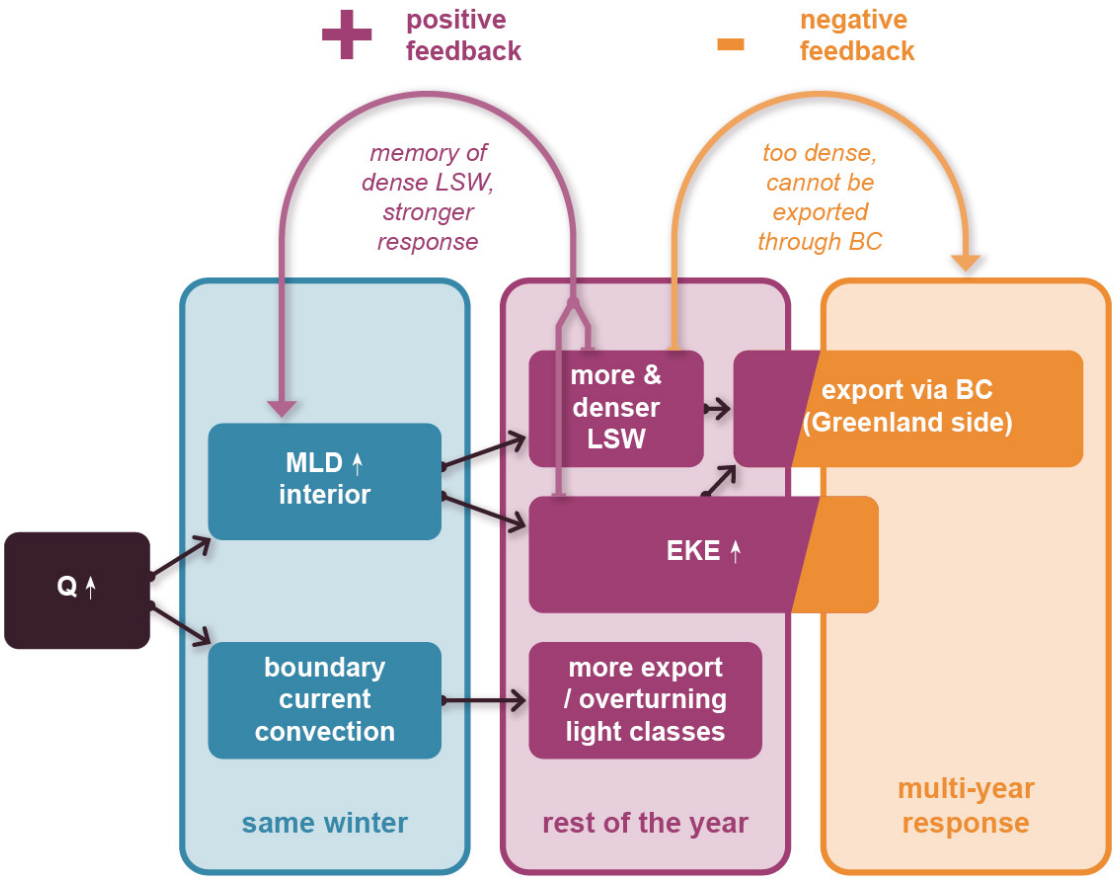

Figure 6.1: Summary of how changes in the heat loss affect the governing processes in the Labrador Sea. The interactions between processes (shown as arrows) and on what timescale these occur (shown as colored boxes) are schematised. The blue, purple and orange boxes indicate the response time of winter surface heat loss, respectively in the same winter, on the remainder of that year, and on the subsequent years. The purple and orange arrow indicate a positive and negative feedback response.

References

Brüggemann, N., & Katsman, C. A. (2019). Dynamics of downwelling in an eddying marginal sea: Contrasting the eulerian and the isopycnal perspective. *Journal of Physical Oceanography*, *49*(11), 3017 - 3035. Retrieved from https://journals.ametsoc.org/view/journals/phoc/49/11/jpo-d-19-0090.1.xml doi: 10.1175/JPO-D-19-0090.1

Caesar, L., Mccarthy, G. D., Thornalley, D. J. R., Cahill, N., & Rahmstorf, S. (2021). Current atlantic meridional overturning circulation weakest in last millennium. *Nature Geoscience*, *14*(3), 118–120. doi: 10.1038/s41561-021-00699-z

Courtois, P., Hu, X., Pennelly, C., Spence, P., & Myers, P. G. (2017). Mixed layer depth calculation in deep convection regions in ocean numerical models. *Ocean Modelling*, *120*, 60-78. Retrieved from https://www.sciencedirect.com/science/article/pii/S146350031730152X doi: https://doi.org/10.1016/j.ocemod.2017.10.007

Gelderloos, R., Katsman, C. A., & Drijfhout, S. S. (2011). Assessing the roles of three eddy types in restratifying the labrador sea after deep convection. *Journal of Physical Oceanography*, *41*(11), 2102 - 2119. Retrieved from https://journals.ametsoc.org/view/journals/phoc/41/11/jpo-d-11-054.1.xml doi: 10.1175/JPO-D-11-054.1

Georgiou, S., Ypma, S. L., Brüggemann, N., Sayol, J.-M., Pietrzak, J. D., & Katsman, C. A. (2020). Pathways of the water masses exiting the labrador sea: The importance of boundary–interior exchanges. *Ocean Modelling*, *150*, 101623. Retrieved from https://www.sciencedirect.com/science/article/pii/S1463500319303385 doi: https://doi.org/10.1016/j.ocemod.2020.101623

Griffies, S. M., & Hallberg, R. W. (2000). Biharmonic friction with a smagorinsky-like viscosity for use in large-scale eddy-permitting ocean models. *Monthly Weather Review*, *128*(8), 2935 - 2946. Retrieved from https://journals.ametsoc.org/view/journals/mwre/128/8/1520-0493_2000_128_2935_bfwasl_2.0.co_2.xml doi: 10.1175/1520-0493(2000)128<2935:BFWASL>2.0.CO;2

Hersbach, H., Bell, B., Berrisford, P., Hirahara, S., Horányi, A., Muñoz-Sabater, J., ... others (2020). The era5 global reanalysis. *Quarterly Journal of the Royal Meteorological Society*, *146*(730), 1999–2049.

Holliday, N. P., Bacon, S., Cunningham, S. A., Gary, S. F., Karstensen, J., King, B. A., ... Mcdonagh, E. L. (2018). Subpolar north atlantic overturning and gyre-scale circulation in the summers of 2014 and 2016. *Journal of Geophysical Research: Oceans*, *123*(7), 4538-4559. Retrieved from https://agupubs.onlinelibrary.wiley.com/doi/abs/10.1029/2018JC013841 doi: https://doi.org/10.1029/2018JC013841

Jackson, L. C., Kahana, R., Graham, T., Ringer, M. A., Woollings, T., Mecking, J. V., & Wood, R. A. (2015). Global and european climate impacts of a slowdown of the amoc in a high resolution gcm. *Climate Dynamics*, *45*(11-12), 3299–3316. Retrieved from https://link.springer.com/article/10.1007/s00382-015-2540-2#citeas doi: 10.1007/s00382-015-2540-2

Johnson, H. L., Cessi, P., Marshall, D. P., Schloesser, F., & Spall, M. A. (2019). Recent contributions of theory to our understanding of the atlantic meridional overturning circulation. *Journal of Geophysical Research: Oceans*, *124*(8), 5376-5399. Retrieved from https://agupubs.onlinelibrary.wiley.com/doi/abs/10.1029/2019JC015330 doi: https://doi.org/10.1029/2019JC015330

Katsman, C. A., Spall, M. A., & Pickart, R. S. (2004). Boundary current eddies and their role in the restratification of the labrador sea. *Journal of Physical Oceanography*, *34*(9), 1967 - 1983. Retrieved from https://journals.ametsoc.org/view/journals/phoc/34/9/1520-0485_2004_034_1967_bceatr_2.0.co_2.xml doi: 10.1175/1520-0485(2004)034<1967:BCEATR>2.0.CO;2

Lavender, K., Davis, R., & Owens, W. (2000). Mid-depth recirculation observed in the interior labrador and irminger seas by direct velocity measurements. *Nature, 407(6800)*. doi: https://doi.org/10.1038/35024048

Li, F., Lozier, M., Bacon, S., Bower, A., Cunningham, S., De Jong, M. F., ... Zhou, C. (2021, 05). Subpolar north atlantic western boundary density anomalies and the meridional overturning circulation. *Nature Communications*, *12*, 3002. doi: 10.1038/s41467-021-23350-2

Lilly, J. M., & Rhines, P. B. (2002). Coherent eddies in the labrador sea observed from a mooring. *Journal of Physical Oceanography*, *32*(2), 585 - 598. Retrieved from https://journals.ametsoc.org/view/journals/phoc/32/2/1520-0485_2002_032_0585_ceitls_2.0.co_2.xml doi: 10.1175/1520-0485(2002)032<0585:CEITLS>2.0.CO;2

Lilly, J. M., Rhines, P. B., Schott, F., Lavender, K., Lazier, J., Send, U., & D'Asaro, E. (2003). Observations of the labrador sea eddy field. *Progress in Oceanography*, *59*(1), 75-176. Retrieved from https://www.sciencedirect.com/science/article/pii/S0079661103001460 doi: https://doi.org/10.1016/j.pocean.2003.08.013

Marotzke, J. (2012). A grip on ice-age ocean circulation. *Nature*, *485*(7397), 180–181. doi: 10.1038/485180a

Marshall, J., & Schott, F. (1999). Open-ocean convection: Observations, theory, and models. *Reviews of Geophysics*, *37*(1), 1-64. Retrieved from https://agupubs.onlinelibrary.wiley.com/doi/abs/10.1029/98RG02739 doi: https://doi.org/10.1029/98RG02739

Pickart, R. S., Torres, D. J., & Clarke, R. A. (2002). Hydrography of the labrador sea during active convection. *Journal of Physical Oceanography*, *32*(2), 428 - 457. Retrieved from https://journals.ametsoc.org/view/journals/phoc/32/2/1520-0485_2002_032_0428_hotlsd_2.0.co_2.xml doi: 10.1175/1520-0485(2002)032<0428:HOTLSD>2.0.CO;2

Yashayaev, I., & Loder, J. W. (2017). Further intensification of deep convection in the labrador sea in 2016. *Geophysical Research Letters*, *44*(3), 1429-1438. Retrieved from https://agupubs.onlinelibrary.wiley.com/doi/abs/10.1002/2016GL071668 doi: https://doi.org/10.1002/2016GL071668

Yu, L., Jin, X., & Weller, R. (2008, 01). Multidecade global flux datasets from the objectively analyzed air-sea fluxes (oaflux) project: Latent and sensible heat fluxes, ocean evaporation, and related surface meteorological variables. *OAFlux Project Tech. Rep. OA-2008-01*.

A | Appendix

A.1 Method

The figures from Chapter 2 are presented in this section.

Figure A.1 shows the most important parameters of how the 3yrDoubleHL run is set-up. For details on what the parameters mean, it is suggested to look into the manual of MITgcm.

```
#; ====================
# | Model parameters |
# ====================
#
# Continuous equation parameters
 &PARM01
 tref = 5.367,5.156166667,4.945333333,4.73450,4.523666667,
        4.312833333,4.1020,3.8650,3.6280,3.5375,
        3.447,3.394,3.341,3.3197,3.2984,
        3.2771,3.24618,3.21525,3.19417,3.17308,
        3.15975,3.14642,3.13778,3.12914,3.122715,
        3.11629,3.110055,3.10382,3.0845,3.0707,
        3.0569,3.0088,2.97996,2.95112,2.913095,
        2.87507,2.79207,2.72171,2.67259,2.62347,
 sRef= 40*35.0,
 viscAz=1.E-5,
 viscAh=40.,
 viscA4=0.25e09,
 no_slip_sides=.TRUE.,
 no_slip_bottom=.TRUE.,
 diffKhT=20.,
 diffK4T=0.125e09,
 diffKzT=1.0e-05,
 diffK4S=0.125e09,
 diffKzS=1.0e-05,
 f0=1.16e-4,
 beta=1.4e-11,
 tAlpha=1.7e-4,
 sBeta =0.0,
#gravity=9.81,
 hMixCriteria=-0.3,
 rigidLid=.FALSE.,
 implicitFreeSurface=.TRUE.,
 implicitDiffusion=.TRUE.,
 implicitViscosity=.TRUE.,
 ivdc_kappa=10,
#useCDscheme=.TRUE.,
#useNHMTerms=.TRUE.,
 eosType='LINEAR',
 rhoNil=1028..
 rhoNil=1028.,
 hFacMin=0.05,
 hFacMinDz=50,
#nonHydrostatic=.TRUE.,
 readBinaryPrec=32,
 bottomDragLinear=2.E-4,
 exactConserv=.TRUE.,
 useSingleCpuIO=.TRUE.,
 &

# Elliptic solver parameters
 &PARM02
 cg2dMaxIters=300,
 cg2dTargetResidual=1.E-13,
 cg3dMaxIters=20,
 cg3dTargetResidual=1.E-8,
 &

# Time stepping parameters
 &PARM03
# 1 jr = 31104000
# 6 jr = 186624000
# 11 jr = 342144000
# 16 jr = 497664000
 nIter0=0000691200,
 startTime=311040000,
 endTime=622080000,
# general synch time stepping
 deltaT=450,
# asynch time stepping (not tested)
# deltaTmom=600,
# deltaTtracer=6000,
# deltaTfreesurf=6000,
# deltaTClock =600.0,
 abEps=0.01,
 pChkptFreq=31104000,
 chkptFreq=311040000,
 dumpFreq=31104000,
# cadjFreq=600,
  monitorFreq=31104000,
# periodicExternalForcing=.FALSE.,
 periodicExternalForcing=.TRUE.,
# 1 / 12 months
 externForcingPeriod=2592000.,
 externForcingCycle=311040000.,
 &
# Gridding parameters
 &PARM04
 usingCartesianGrid=.TRUE.,
 delZ= 20,20,20,20,20,
       50,50,50,50,50,
       50,50,50,50,50,
       50,50,50,50,50,
       75,75,75,75,75,
       75,75,75,75,100,
       100,100,100,125,125,
       150,150,150,175,200,
 delX=324*3.75e03,
 delY=420*3.75e03,
 &
# Input datasets
 &PARM05
 bathyFile = 'new_topo_OB_steep_3750.bin',
# uVelInitFile = 'OBzonalU.bin'
 surfQfile = 'Q10file_3yr_100_perc_HL_run_29_3.75km_32bits.bin',
 diffKrFile= 'krfile_3750_32_z40.bin',
 &
```

Figure A.1: The parameters for setting up the numerical model used in 3yrDoubleHL. For details on what the parameters mean, it is suggested to look into the manual of MITgcm.

A.2 EKE and MLD plots

The figures from Section 3.2 are presented in this section. Each figure contains the EKE and MLD per year, based on the winter months (February and March) of respectively REF (Figure A.2), 1yrDoubleHL (Figure A.3) and 5yrDoubleHL (Figure A.4).

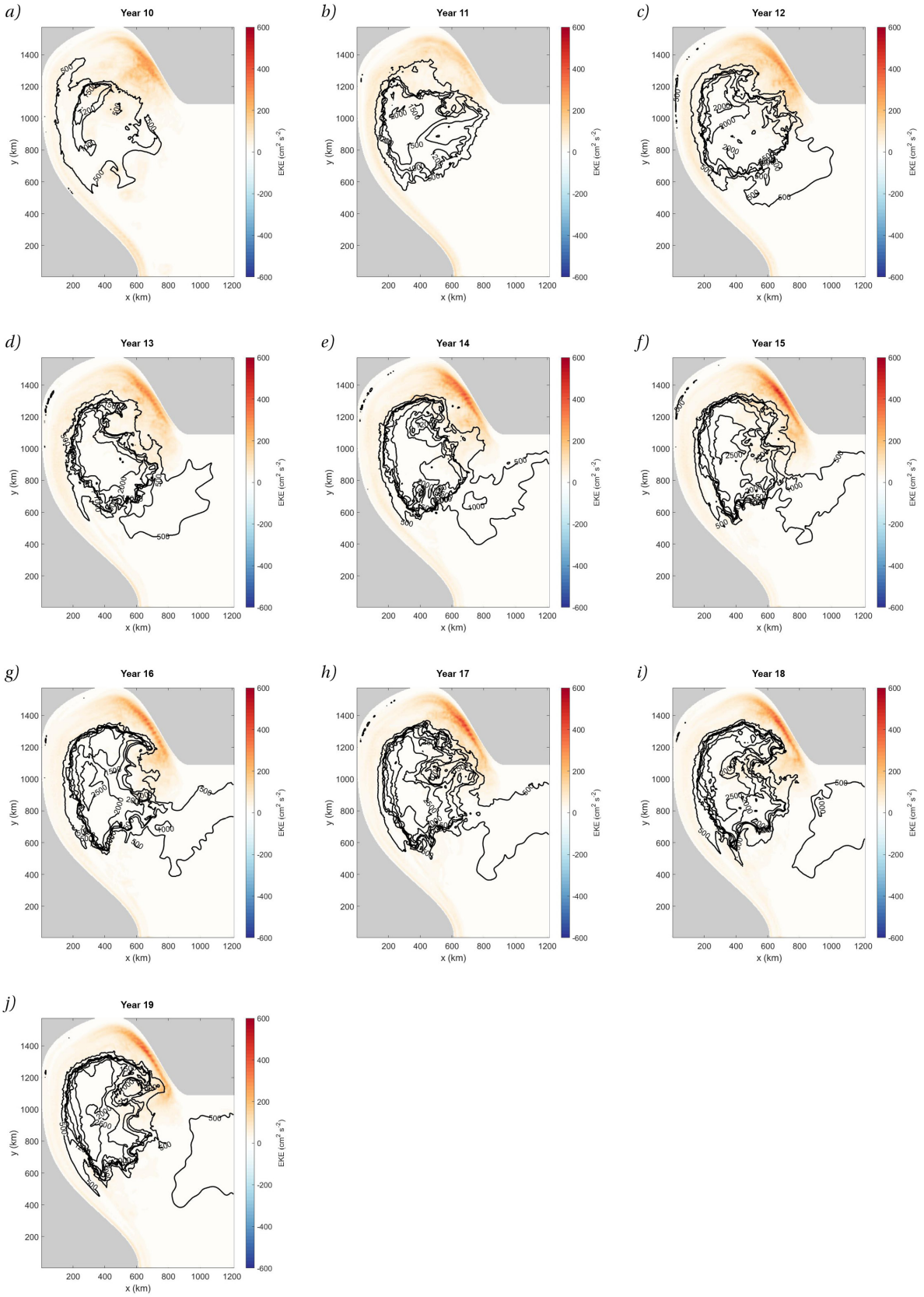

Figure A.2: Mean EKE (shading) and MLD (contours) per year, based on the months February and March for run REF. The MLD is plotted with contour lines in meters, with intervals of 500m. The EKE is shaded and expressed in cm^2/s^2.

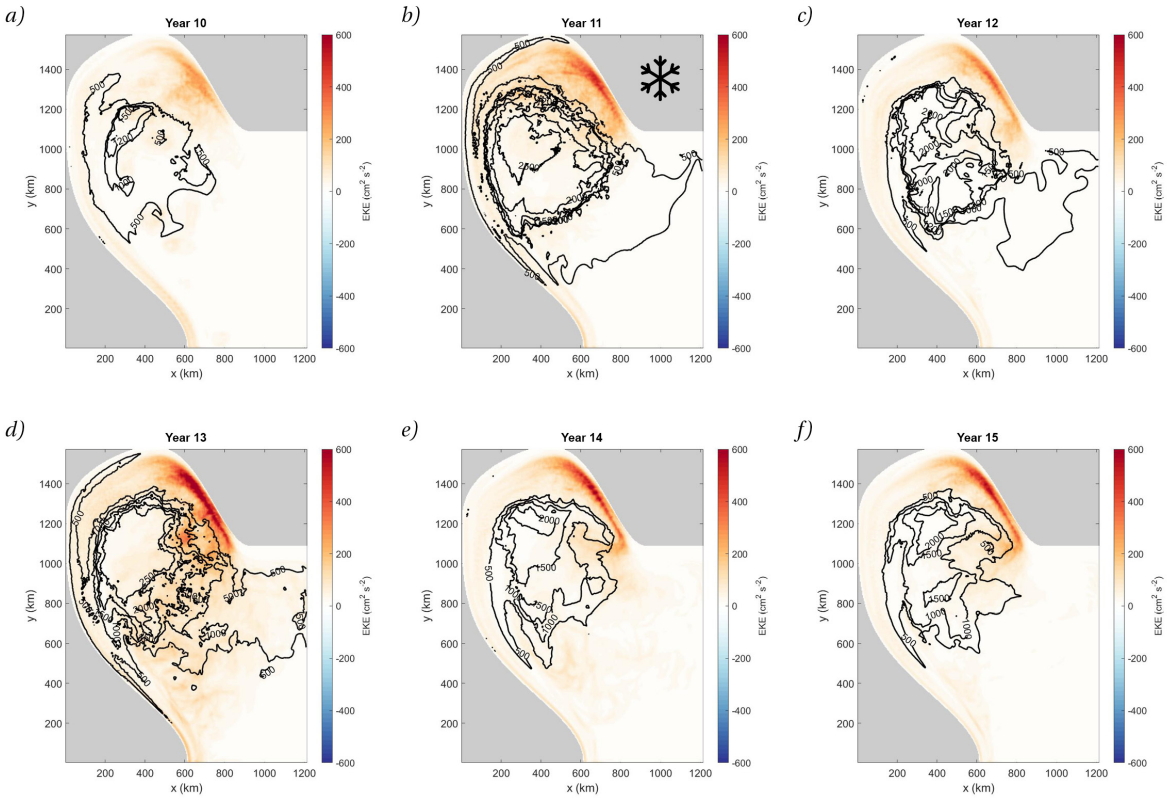

Figure A.3: Mean EKE (shading) and MLD (contours) per year, based on the months February and March for run 1yrDoubleHL. The MLD is plotted with contour lines in meters, with intervals of 500m. The EKE is shaded and expressed in cm^2/s^2. The surface heat loss is double the average surface heat loss in year 11, depicted by a frost sign.

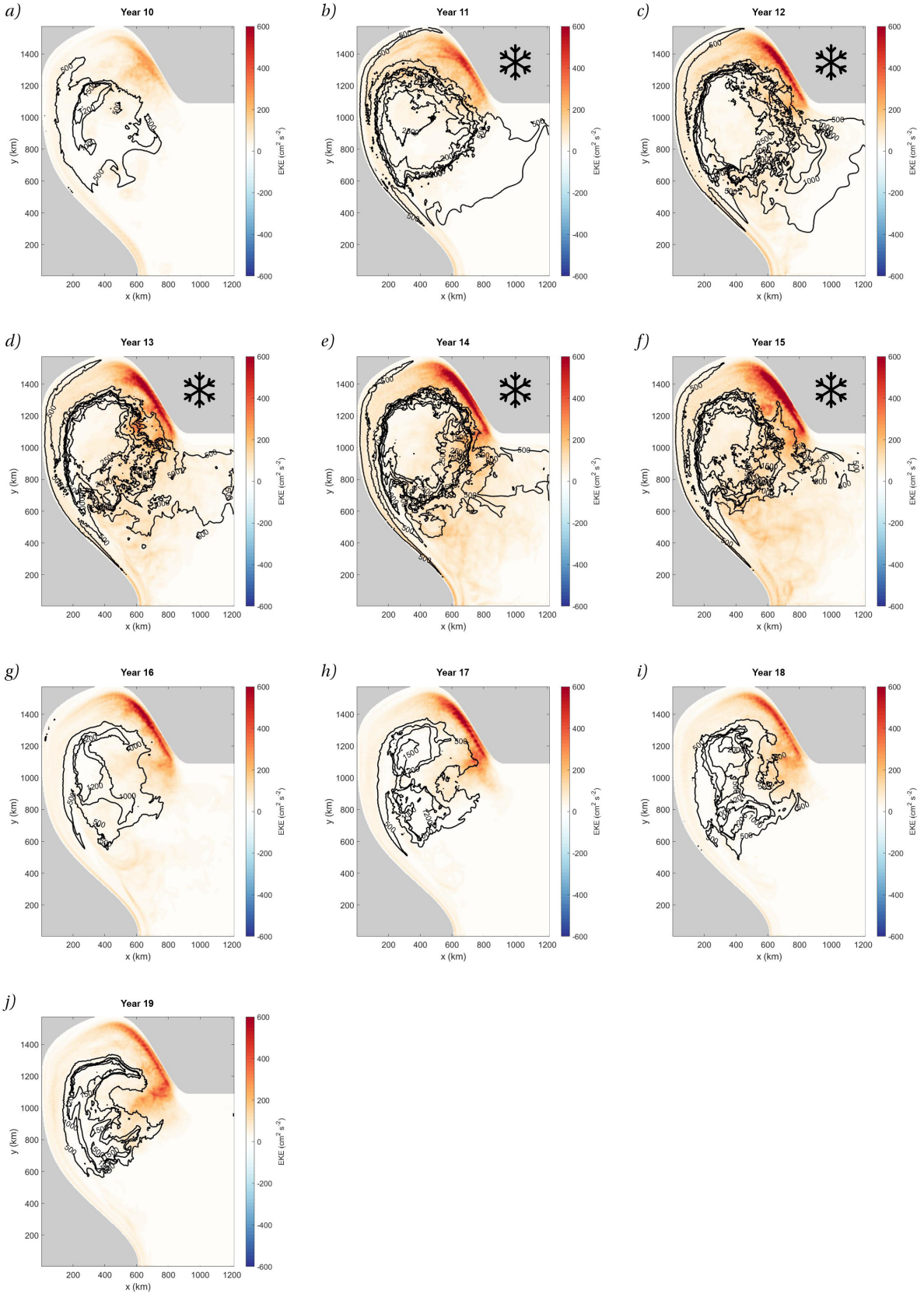

Figure A.4: Mean EKE (shading) and MLD (contours) per year, based on the months February and March for run 5yrDoubleHL. The MLD is plotted with contour lines in meters, with intervals of 500m. The EKE is shaded and expressed in cm^2/s^2. The surface heat loss is double the average surface heat loss in the years 11, 12, 13, 14 and 15 depicted by frost signs.